Distinct Roles for Human Cytomegalovirus Immediate Early Proteins IE1 and IE2 in the transcriptional regulation of MICA and PVR/CD155 expression.

Benedetta Pignoloni[*,1], Cinzia Fionda[*,1], Valentina Dell'Oste[†], Anna Luganini[‡], Marco Cippitelli[*], Alessandra Zingoni[*], Santo Landolfo[†], Giorgio Gribaudo[‡], Angela Santoni[*,§], Cristina Cerboni[*].

[*] Department of Molecular Medicine, Istituto Pasteur-Fondazione Cenci Bolognetti, "Sapienza" University of Rome, Viale Regina Elena 291, 00162 Rome, Italy; [†] Department of Public Health and Pediatric Sciences, University of Turin, Via Santena 9, 10126 Turin, Italy; [‡] Department of Life Sciences and Systems Biology, University of Turin, Via Accademia Albertina 13, 10123 Turin, Italy; [§] I.N.M. Neuromed, Pozzilli, Isernia, Italy.

[1] These authors equally contributed to the work.

Running title

HCMV, IE proteins and regulation of NKG2D/DNAM-1 ligands

Corresponding authors: Cristina Cerboni and Angela Santoni; Phone: +39-0649255128; Fax: +39-0644340632 Email: cristina.cerboni@uniroma1.it; angela.santoni@uniroma1.it

Key words

Human cytomegalovirus, IE proteins, NKG2D and DNAM-1 ligands.

Abstract

Elimination of virus-infected cells by cytotoxic lymphocytes is triggered by activating receptors, among which NKG2D and DNAM-1/CD226 play an important role. Their ligands - MICA/B and ULBP1-6 (NKG2DL), Nectin-2/CD112 and PVR/CD155 (DNAM-1L) - are often induced on virus-infected cells, though some viruses, including Human Cytomegalovirus (HCMV), can block their expression. Here, we report that infection of different cell types with laboratory or low-passage HCMV strains upregulated MICA, ULBP3 and PVR, with NKG2D and DNAM-1 playing a role in NK cell-mediated lysis of infected cells. Inhibition of viral DNA replication with phosphonoformic acid did not prevent ligand upregulation, thus indicating that early phases of HCMV infection are involved in ligand increase. Indeed, the major immediate early (IE) proteins IE1 and IE2 stimulated the expression of MICA and PVR, but not ULBP3. IE2 directly activated *MICA* promoter, via its binding to an IE2-responsive element we identified within the promoter, and that is conserved among different alleles of *MICA.* Both IE proteins were instead required for PVR up-regulation, via a mechanism independent of IE DNA-binding activity. Finally, inhibiting IE protein expression during HCMV infection confirmed their involvement in ligand increase. We also investigated the contribution of the DNA damage response (DDR), a pathway activated by HCMV and implicated in ligand regulation. However, silencing of ATM, ATR and DNA-PK kinases did not influence ligand expression. Overall, these data reveal that MICA and PVR are directly regulated by HCMV IE proteins, and this may be crucial for the onset of an early host anti-viral response.

Introduction

Human cytomegalovirus (HCMV) is an endemic β-herpesvirus that does not cause clinically obvious disease in healthy individuals, where it establishes a life-long latency. In immunocompromised hosts, such as AIDS patients and organ transplant recipients, infection often becomes clinically apparent and can cause life-threatening diseases. HCMV is also the leading viral cause of congenital infections and birth defects (1,2). HCMV disseminates throughout the body, with a broad range of different cell types supporting productive viral infection (3). In addition, it induces a plethora of immunomodulatory pathways to subvert the host innate and adaptive immune responses (2). To date, few anti-viral drugs are available, but long-term treatment is frequently associated with toxic side effects and the emergence of drug-resistant mutants (4,5).

Clearly, in the absence of an effective and preemptive HCMV vaccine, additional therapeutic agents are urgently needed, and strategies to potentiate anti-HCMV immune response could be also a valuable alternative approach.

With this rationale, we investigated whether molecules capable of activating cytotoxic lymphocytes may be positively regulated following HCMV infection, thus enhancing the recognition and elimination of infected cells. In particular, we focused on the ligands of NKG2D and DNAM-1/CD226, two activating receptors expressed by all cytotoxic lymphocytes. NKG2D delivers a potent activating signal and plays a prominent role in the recognition and elimination of infected cells (6,7). In humans, NKG2D ligands (NKG2DL) are the MHC-I-related molecules MICA, MICB, and the ULBP proteins (ULBP1-6), whose expression is restricted in normal cells, but it can be rapidly induced upon cellular stress, including a viral infection (6,7). DNAM-1 receptor is essential to NK cell-dependent anti-tumor immunity (8) and its role in the response to viral infections is also starting to emerge (9-12). It is an adhesion molecule and the binding to its ligands, Poliovirus Receptor (PVR) (CD155) and Nectin-2 (CD112), promotes leukocyte migration, as well as effector responses of both NK and T cells (8,13). HCMV evolved specific strategies

to block the functions of NKG2D and DNAM-1. Indeed, there is an array of viral molecules (UL16, UL141, UL142, US18 and US20, US9, miRNA-UL112) targeting both NKG2DL and DNAM-1L, and impairing recognition and elimination of HCMV-infected cells by NK cells and other NKG2D+ and DNAM-1+ cells (14-17). In contrast, it is still debated if and how HCMV up-regulates NKG2DL, while for DNAM-1L it has not been investigated.

IE proteins are the first to be expressed during HCMV lytic infection and play crucial roles in regulating viral gene expression and in dysregulating host cell physiology, to dictate an intracellular environment conducive to viral replicative cycle, as well as in counteracting host immune responses (2). The 72-kDa IE1, 86-kDa IE2 and 55-kDa IE55 proteins share identical N-terminal 85 amino acids resulting from differentially spliced transcripts, and their expression does not require *de novo* protein synthesis (18,19). IE1 and IE2 are absolutely critical for the temporal cascade of viral gene expression, as they transactivate E and L genes, and either positively or negatively autoregulate their own expression (18,19). While IE1 is a relatively weak transactivator, IE2 is the most important HCMV regulatory protein and is a strong transcriptional activator of viral and cellular gene expression. It binds to DNA directly, represses its own promoter (the Major IE Promoter; MIEP) (20), and cooperates with cellular transcription factors via protein-protein interactions. These IE2 activities are crucial for transcriptional activation of viral and host genes, as well as for regulation of several cellular functions (19). The IE55 protein is a splice variant of IE2 gene product, with a deletion between residues 365 and 519 in the C-terminus, a region required for many IE2 functions, including transcriptional activation and DNA binding (19,21-25).

Among the cellular pathways activated by IE proteins there is the DNA damage response (DDR) (26,27), involved in cell-cycle checkpoint control, DNA replication and repair, and apoptosis (28). DDR is activated by many viruses, including HCMV, and although its functional relevance in HCMV infection has not been clarified, this virus induces DDR, including activation of ATM, ATR and the downstream

protein H2AX (26,27,29-34). Interestingly, expression of some NKG2DL and DNAM-1L can be dependent on the activation of DDR and on ATM/ATR kinases (35-43).

Here, we investigated the role and the mechanisms of IE protein-mediated regulation of NKG2DL and DNAM-1L, as well as the potential of DDR in stimulating activating ligand expression. This study provides new mechanistic insight into the regulation of anti-viral immunity by HCMV IE proteins.

Materials and methods

Antibodies and reagents

The following mAbs were used in flow cytometry: anti-MICA (M673) and anti-ULBP4 (M475) (Amgen); anti-MICA (AMO-1) (BamOmaB); anti-MICB (MAB236511), anti-ULBP1 (MAB170818), anti-ULBP2 (MAB165903), and anti-ULBP3 (MAB166510) (R&D Systems); anti-Nectin-2 (CD112) and mouse control IgG_1-Fluorescein isothiocyanate (FITC) (BD Biosciences); anti-PVR (SKII.4) kindly provided by Dr M. Colonna (Washington University, St Louis, MO); Alexa fluor 488-conjugated anti-IE antigens (MAB810X) and FITC-conjugated anti-phospho-histone H2AX (γH2AX) (Ser139; clone JBW301) (Merck Millipore); mouse control IgG (Biolegend); allophycocyanin (APC)-conjugated goat anti-mouse (GAM) (Jackson Immunoresearch Laboratories); GAM-FITC (Cappel). In cytotoxicity assays, the following blocking mAbs were used: anti-NKG2D (MAB149810, R&D Systems), anti-DNAM-1 (clone DX11, Bio-Rad), and mouse IgG1 isotype control (Biolegend). The following antibodies were used in immunoblotting: anti-p85 subunit of PI-3 kinase and anti-IE antigens (MAB810R) (Merck Millipore); anti-ATM (D2E2) (Cell Signaling Technology); anti-ATR (sc-1887), anti-DNA-PK_{CS} (sc-5282) (Santa Cruz). Other reagents used were: caffeine, methylcellulose, phosphonoformic acid (PFA) (Foscarnet), gelatin and crystal violet (Sigma Aldrich); Lipofectamine 2000 (Invitrogen), Dharmafect from Dharmacon (GE Healthcare). The phosphorothioate oligodeoxynucleotide fomivirsen (also known as ISIS 2922) complementary to IE2 mRNA (44,45) was synthesized by Metabion International AG.

Cells and culture conditions

Primary human foreskin fibroblasts (HFFs), the retinal epithelial cell line ARPE-19 and the human embryo kidney 293T cells were purchased from the American Type Culture Collection. HFF and 293T cells were grown in DMEM containing 10% FCS, 2 mM glutamine, 1 mM sodium pyruvate, 100 U/ml penicillin, and 100 µg/ml streptomycin sulfate, and ARPE-19 cells in a 1:1 mixture of DMEM and Ham's

F-12 medium (Invitrogen) containing 10% FCS, 15 mM HEPES, 2 mM glutamine, 1 mM sodium pyruvate, 100 U/ml penicillin, and 100 μg/ml streptomycin sulfate. HFFs were used at passages 14 to 28. Human dermal microvascular endothelial cells (HMVECs) (CC-2543) were obtained from Clonetics, and cultured in endothelial growth medium corresponding to endothelial basal medium (Clonetics), containing 10% FCS, human recombinant vascular endothelial growth factor, basic fibroblast growth factor, human epidermal growth factor, insulin growth factor 1, hydrocortisone, ascorbic acid, and heparin. Cells were seeded onto culture dishes coated with 0.2% gelatin. Experiments were carried out with cells at passages 4 to 15. Fibroblasts derived from an ataxia-telangectasia mutated patient and not expressing ATM protein (AT-/-), were kindly provided by Drs. M. Fanciulli and T. Bruno (Regina Elena National Cancer Institute, Rome, Italy) (46). They were grown in DMEM containing 15% FCS and used at passages 5 to 8. All cells were maintained at 37°C in a 5% CO_2 atmosphere.

HCMV preparations and infection conditions

The HCMV AD169 strain (ATCC-VR538) was prepared by infecting semi-confluent monolayers of HFF cells at a virus-to-cell ratio of 0.01, and cultured until a marked cytopatic effect was seen. Stocks were then prepared after 3 rounds of cell freezing and thawing, subjected to centrifugal clarification, and frozen at −80°C. Virus titers were measured by standard plaque assays on HFF cells. Stock solutions used in all experiments contained approximately $2x10^7$ PFU/ml. Standard plaque assays were used also in different experiments to determine viral titers in the supernatants harvested from infected cells. HCMV TR was derived from an ocular specimen (47), and after a few passages on fibroblasts, was cloned into a BAC (48,49). Reconstitution of infectious TR was performed as previously described (50) by co-transfecting HFFs with the corresponding TR BAC and a plasmid expressing HCMV pp71. Reconstituted infectious virus retained the ability to infect endothelial and epithelial cells, as well as monocytes and macrophages (49,50). HCMV VR1814 is a derivative of a clinical isolate recovered from a cervical swab of a pregnant

144 woman (51). This strain was propagated in HUVEC and titrated as previously described (52).
145 Cells were infected at about 80-90% confluence at a molteplicity of infection (MOI) of 1 PFU/cell, unless
146 otherwise specified, in their respective culture medium, without FCS, and after 2 h (AD169 or TR strains)
147 or 5 h (VR-1814 strain) at 37°C, virus inoculum was discarded and replaced with fresh growth medium
148 (day 0). Mock-infected control cultures were exposed for the same amount of time to an equal volume of
149 medium. At various dpi, cells were harvested and analyzed. In some experiments, PFA was added after
150 virus inoculation at a final concentration of 200 μg/ml, while fomivirsen was added 1 h before viral
151 inoculum, maintained in the culture medium during the infection and then throughout the assay (44,45).
152 The DDR inhibitor caffeine (53,54) was added 2 dpi at a final concentration of 10 mM.
153
154 **Adenovirus vectors and infections**
155 Recombinant adenoviruses (AdV) encoding HCMV IE2 (AdV-IE2) and *E. coli* β-galactosidase (AdV-
156 LacZ) have been previously described (55,56), while AdV-IE72 (AdV-IE1) was kindly provided by Dr.
157 Timothy F. Kowalik (University of Massachusetts Medical School, Worcester, USA) (27). Recombinant
158 AdV stocks were generated, purified and titrated as previously described (27,55,56). For adenoviral
159 transduction, HFFs were infected at about 80-90% confluence at an MOI of 4 PFU/cell in DMEM
160 without FCS, for 2 h at 37°C. When the viral proteins were not expressed in combination, the total MOI
161 was equalized to 4 with AdV-LacZ. After 2 h, the virus inoculum was discarded and replaced with fresh
162 growth medium (day 0) and analyzed at the indicated dpi. Mock-infected cells served as control cultures.
163 Following infection, cultures were maintained in growth medium and analyzed at the indicated dpi.
164
165 **Immunofluorescence and FACS analysis**
166 Mock-infected or infected cells were harvested at the indicated dpi and stained with mAbs specific for
167 MICA, MICB, ULBP1-4, PVR and Nectin-2, followed by GAM-APC or by GAM-FITC (for experiments

with PFA), and analyzed by flow cytometry on an FACSCalibur (Becton Dickinson). The mean of fluorescence intensity (MFI) value of the isotype control antibody was always subtracted from the MFI relative to each molecule. For intracellular staining of IE antigens or phosho-histone H2AX (γH2AX), cells were fixed in 1% formaldehyde, permeabilized with 70% ethanol, and then incubated with Alexa fluor 488-conjugated anti-IE mAb (MAB810X) or with FITC-conjugated anti-γH2AX (JBW301), respectively.

Cytotoxicity assays

Cell-mediated cytotoxicity was assessed in 4-h ^{51}Cr release assays. Polyclonal NK cells, generated as previously described (57) were used as effectors, and incubated at different ratios with $5x10^3$ target cells in U-bottom, 96-well microtiter plates at 37°C in a 5% CO_2 atmosphere. To block NKG2D and DNAM-1 receptors, effector cells were preincubated with 1 μg/10^6 cells of specific or isotype control mAbs for 15 min at room temperature. Cells were then washed and used in the assays. Percentage of lysis was determined by counting an aliquot of supernatant and using the formula: 100 x [(sample release - spontaneous release)/(total release - spontaneous release)]. Mean inhibition of lysis (%) ± SE by anti-NKG2D, anti-DNAM-1 or isotype control mAb treatment was calculated in comparison to untreated NK cells (no Ab) using the formula: [1- (% specific lysis by mAb treatment / % specific lysis of no Ab) x 100].

Immunoblot analysis

Cells were lysed for 20 minutes at 4°C in a lysis buffer containing 0.2% Triton X-100, 0.3% NP40, 1 mM EDTA, 50 mM Tris HCl pH 7.6, 150 mM NaCl, and protease inhibitors to obtain whole-cell protein extracts. Lysates (30-40 μg) were resolved by SDS-PAGE and transferred to nitrocellulose membranes (Merck Millipore). Membranes were blocked with 5% milk and probed with the indicated antibodies.

Immunoreactivity was revealed using an enhanced chemiluminescence kit (Amersham).

siRNA

The ON-TARGETplus SMARTpool siRNA specific for ATM and ATR (siATM, siATR), and the ON-TARGETplus non-targeting pool (siCtrl) were purchased from Dharmacon (Thermo Fisher Scientific). siRNA specific for DNA-PK_{CS} (sc-35200) (siDNA-PK) was from Santa Cruz. HFFs (70%-80% confluence) were transfected with 100-200 nM of siRNA using DharmaFECT siRNA Transfection Reagent (Thermo Fisher Scientific), according to the manufacturer's recommendations. One to two days after transfection, cells were infected with AD169, as indicated in the figure legends. Cells and supernatants were harvested and analyzed at 2 or 3 dpi, as indicated. Densitometric analysis was performed with ImageJ software.

RNA isolation and real-time PCR

Total RNA was extracted using TRI Reagent Solution (Life Technologies), according to manufacturer's instructions, and 1 µg of total RNA was used for cDNA first-strand synthesis in a reaction volume of 25 µl. Real-Time PCR was performed using the ABI Prism 7900 Sequence Detection system (Applied Biosystems); cDNAs were amplified in triplicate with primers for MICA (Hs00792195_m1), ULBP3 (Hs00225909_m1), (PVR (Hs00197846_m1), and GAPDH (Hs03929097_g1), using specific TaqMan Gene Expression Assays (Applied Biosystems). Relative expression of each gene versus GAPDH was calculated according to the $2^{-\Delta\Delta Ct}$ method.

Plasmids, transfections and chromatin immunoprecipitation assays (ChIP)

The pGL3-*MICA* promoter vector was previously described (58) and kindly provided by Dr. J. Bui (University of California at San Diego, La Jolla, CA). The *MICA* -270 promoter plasmid was obtained as

previously described (59). Mutant *MICA* -270-CG construct was generated using Quick Change Site-Directed Mutagenesis Kit (Stratagene). Primer sequences used were: -92 bp -CGGTCGGGGGACCG -78 bp; primers for mutagenesis: for 5' -CCAGTTTCATTGGATGAGATGTCGGGGGACATGGCCAGGTGACTAAG-3'; rev 5'-CTTAGTCACCTGGCCATGTCCCCCGACATCTCATCCAATGAAACTGG-3'. Inserted mutations were verified by sequencing. pGL2-*PVR* (-571 bp fragment) promoter luciferase reporter vector and progressive deletions were kindly provided by Dr. G. Bernhardt (Hannover Medical School, Hannover, Germany) (60). pSG5-IE1, pSG5-IE2, and pSG5-IE55 were previously described (24). The IE2 cDNA cloned in the pRSV vector and the zinc finger mutant of IE2, with cysteines 428 and 434 mutated into serine residues (pRSV-IE2-Zn mut), were a generous gift of Prof. Jay Nelson (61).

In all transfection experiments, 3 µg of luciferase reporter, 0.25 µg of pRL-CMV-Renilla, and 2 µg of IE protein vectors or pSG5 empty vector were co-transfected into 80-90% confluent cells growing on a 10 cm^2 area using Lipofectamine 2000 (Invitrogen) according to the manufacturer's protocols. In some experiments, the pSG5-IE2 vector was replaced by pSG5-IE55, pRSV-IE2 or pRSV-IE2-Zn-mut, as indicated. 48 h post-transfection, cells were harvested and prepared for the luciferase assays, using the Dual-Luciferase Reporter Assay kit and the Glomax Multi Detection System (Promega), following the manufacturer's instructions. Relative luciferase activity was calculated by dividing the luciferase activity of pGL3-*MICA* or pGL2-*PVR* reporter, co-transfected with IE proteins, by the respective pGL3- or pGL2-Basic, to remove the unspecific effect of IE proteins on the reporter vector. The unspecific modulation of the reporter empty vector activity was probably due to a general activation of the transcriptional machinery by IE proteins, and was more evident for IE1. This correction allowed us to better appreciate the specific effect of the viral proteins on ligand promoters.

In ChIP assays, 293T cells were co-transfected with 5 µg of *MICA* -270 promoter plasmid, wild-type or mutated, and pSG5-IE1 (10 µg) and pSG5-IE2 (10 µg), or pSG5 empty vector (20 µg), using

Lipofectamine 2000. In ChIP assays on the endogenous *MICA* promoter, 293T cells were transfected with pSG5-IE1, pSG5-IE2, or pSG5 empty vector. After 48 h, cells were processed for ChIP assays following the manufacturer's protocol of Magna ChIP AG chromatin immunoprecipitation kit (Merck Millipore). Chromatin was immunoprecipitated with a polyclonal rabbit anti-IE antibody, recognizing a segment of IE2 (amino acids 1-143), or control polyclonal rabbit serum. PCR primers used were: MICA for 5′-AGGTCTCCAGCCCACTGGAATTTTCTC-3′; MICA rev 5′-CGCCACCCTCTCAGCGGCTCAAGC-3′. Results are expressed as relative enrichment as compared to the input. Negative control (polyclonal rabbit serum) values were subtracted from the corresponding samples. Quantifications were obtained by serial dilutions of the input DNA samples. The analysis was performed using the SDS version 2.4 software (Applied Biosystems). PCRs were validated by the presence of a single peak in the melt curve analysis, and amplification of a single specific product was further confirmed by electrophoresis on agarose gel.

Confocal microscopy analysis

For staining of cell surface MICA, HFFs were grown to semi-confluence on glass coverslips in 24-well plates and infected with AD169 and TR at a MOI of 1 PFU/cell for 2 h at 37°C. After 4 dpi, cells were washed with PBS, fixed in 1% paraformaldehyde for 15 min at room-temperature (RT), blocked in 1% FCS diluted in PBS (20 min., RT), but not permeabilized. Indirect immunofluorescence analysis was performed by incubating fixed cells with the anti-MICA mAb AMO-1 (1:40) for 2 h at 37°C, followed by secondary antibody incubation with CF594-conjugated rabbit anti-mouse IgG (Sigma) for 1 h at RT. Samples were then visualized with an Olympus IX70 inverted laser scanning confocal microscope, and images were captured using FluoView 300 software (Olympus Biosytems).

Statistical analysis

Statistical analysis of the data was performed using a paired Student *t*-test, or a one-way analysis of variance (ANOVA), where indicated. *: $p<0.05$; **: $p<0.01$; ***: $p<0.001$; ****: $p<0.0001$.

Results

Regulation of NKG2D and DNAM-1 ligand expression by different HCMV strains.

Increased or *de novo* expression of T/NK cell activating ligands on infected cells represents a crucial host immune defense mechanism to sense and react against different pathogens (7,12). Therefore, we examined the expression of NKG2DL and DNAM-1L in several cell models with multiple HCMV strains. Firstly, human primary foreskin fibroblasts (HFFs) were infected with the HCMV laboratory strain AD169. We observed higher levels of MICA and ULBP3 on infected HFFs, with maximal expression around 3 dpi, whereas no changes in MICB, ULBP1 or ULBP4 expression were detected. In contrast, ULBP2 was down-modulated by HCMV (Figure 1). The DNAM-1L PVR, but not Nectin-2, was also up-regulated by HCMV, with a maximal increase at 3 dpi (Figure 1).

To verify that the augmented expression of MICA, ULBP3 and PVR was not restricted to a particular viral strain, their modulation was also examined in HFFs infected with the low-passage strains VR-1814 and TR. Consistently, an induction of MICA was observed upon infection with VR-1814, independently of the MOI (Fig. 2A-B). Low, but statistically significant level of MICA induction was also observed with TR (Fig. 2C), and was confirmed by confocal microscopy (Fig. S1). ULBP3 and PVR ligands were also up-regulated on HFFs infected with VR-1814 (Fig. 2A-B) or TR (Fig. 2C). Taken together, these results demonstrated that by 3-4 dpi, MICA, ULBP3 and PVR were up-regulated on infected primary fibroblasts in a HCMV strain-independent manner.

Next, we extended our investigation to other cell type-viral strain combinations, by infecting primary endothelial (HMVEC) and epithelial cells (ARPE-19) with TR and VR-1814 strains (Figure 2C). MICA expression was either down-modulated on TR-infected HMVECs, or not affected in the other combinations, while ULBP3 and PVR were always up-regulated, independently of the cell type and/or the viral strain used.

Thus, these results demonstrate that, despite few exceptions, HCMV positively regulates the expression

of MICA, ULBP3 and PVR activating ligands, with a pattern that generally overcome cellular- or viral strain-related differences.

NKG2D and DNAM-1 ligands contribute to the NK cell-mediated killing of infected fibroblasts.

Next, we tested whether the observed upregulation of NKG2D and DNAM-1 ligands upon HCMV infection had consequences on NK cell-mediated cytotoxicity. Chromium-release assays were performed using polyclonal NK cell cultures from different donors as effectors, and uninfected or AD169- and TR-infected HFFs as targets. HFFs infected with the low-passage strain TR became more resistant to NK cell-mediated lysis, while infection with AD169 resulted in a variable pattern, with an either increased, unchanged or decreased sensitivity (Fig. 3A and data not shown). These results are in line with previous observations on both laboratory and low-passage HCMV strains, which demonstrated that cells infected with low-passage strains were more resistant to NK cell-mediated cytotoxicity, compared to AD169-infected cells (14,15,57,62). Nevertheless, despite the increased resistance of TR-infected cells to NK cell lysis, blocking NKG2D or DNAM-1 receptors resulted in a significant inhibition, that was comparable to that observed with AD169-infected cells or uninfected cells, in all experiments performed (Fig. 3B).

Overall, these data indicate that NKG2D and DNAM-1 receptors contribute to the elimination of HCMV-infected cells. Moreover, despite the increased resistance to NK lysis of HFFs infected with the TR strain, NKG2D and DNAM-1 ligands still contribute to the recognition of these target cells, in accordance with the increased expression of MICA, ULBP3 and PVR ligands upon TR infection.

Role of the DDR and of ATM, ATR and DNA-PK on HCMV-induced ligand up-regulation.

As previous studies reported that HCMV manipulates the DDR (26,27,29-34), a pathway able to stimulate NKG2DL and DNAM-1L expression as well (35-43), we examined the involvement of DDR

signaling in the HCMV-mediated up-regulation of activating ligands, using genetic and pharmacological approaches.

Upon HCMV infection, the levels of γH2AX, the phosphorylated form of the histone variant H2AX, a well-known substrate of DDR kinases (28), increased of approximately two-fold, demonstrating activation of the DDR pathway in our experimental settings (Fig. S2A-B). Next, we determined the contribution of the three main DDR kinases (ATM, ATR and DNA-PK) on ligand expression, IE expression and viral replication. Firstly, the role of ATM was investigated in fibroblasts derived from a patient affected by ataxia-telangiectasia (AT-/-), where ATM is not detectable. HCMV infection still increased the expression of MICA, ULBP3 and PVR, though with delayed kinetics compared to normal HFFs (Fig. S2C). Moreover, both progeny virus production and IE expression were only partially affected in AT-/- cells, but not in a statistically significant manner (data not shown). Then, we used specific siRNA to transiently deplete ATM (siATM) (Fig. S2D-G), and consistently to AT-/- fibroblasts, there was no effect on MICA, ULBP3 and PVR expression induced by HCMV (Fig. S2D), and on the percentage of IE+ cells and viral replication (Fig. S2E-F). Similar results were obtained with siRNA specific for ATR (Fig. S3A-D) or DNA-PK (Fig. S3E-H), as well as with a triple gene silencing with the three siRNA specific for ATM, ATR and DNA-PK (siDDR) (Fig. 4). Finally, activating ligands were still up-regulated in AD169-infected HFFs treated with caffeine, a well-known and broad spectrum inhibitor of DDR (data not shown).

Altogether, these results suggest that DDR activation does not play a role in the HCMV-induced up-regulation of MICA, ULBP3 and PVR.

The HCMV-induced ligand increase depends on events occurring prior to the onset of viral DNA replication and involves transcriptional activation.

To identify the molecular mechanisms underlying ligand up-regulation in HCMV-infected cells, we

hypothesized that some events in the early stages of infection could be responsible. To verify this hypothesis, HFFs were infected with HCMV and treated with phosphonoformic acid (PFA), a selective inhibitor of viral DNA polymerase (63). As shown in Fig. 5, MICA, ULBP3 and PVR levels were increased on the surface of infected cells even in the presence of PFA, indicating that viral DNA replication and expression of delayed-E and L genes are dispensable for ligand up-regulation.

Next, to investigate whether the increase in ligand cell surface levels was a consequence of a virus-induced transcriptional activation, we measured ligand mRNA content by real-time PCR at different hours post-infection (hpi). MICA, ULBP3 and PVR mRNA progressively increased during the course of infection, with a maximal expression at 24-48 hpi (Fig. 6).

These data suggest that up-regulation of MICA, ULBP3 and PVR cell surface levels by HCMV is the outcome of a transcriptional activation of the corresponding genes.

HCMV IE proteins up-regulate MICA and PVR gene expression.

Because early steps of infection were crucial for ligand up-regulation, we investigated if the major viral IE proteins, IE1 and IE2, were involved in the modulation of MICA, ULBP3 and PVR expression, by transducing HFFs with recombinant adenoviruses (AdV) encoding for IE1, IE2, or their combination, and analyzing ligand mRNA and cell surface levels at 24, 48 and 72 hpi. There was a significant up-regulation of MICA mRNA at all time points only in IE2 transduced cells, while IE1 did not affect MICA mRNA levels, neither when used alone nor in combination with IE2 (Fig. 7A). Similar results were obtained for MICA cell surface expression, which showed an IE2-dependent increase, particularly evident at 72 hpi (Fig. 7B-C and data not shown). In contrast, PVR mRNA content and membrane expression was mostly up-regulated by the co-expression of IE1 and IE2, while IE proteins alone had weaker effect (Fig. 7A-C). ULBP3 mRNA and cell surface expression were instead not affected by IE proteins (Fig. S4). Thus, while the HCMV-induced up-regulation of ULBP3 may be the consequence of other virus-related

362 effects than the solely overexpression of IE1/IE2, MICA and PVR increase could be reproduced by
363 expression of IE proteins, though with different requirement.
364 Then, to further sustain the role of IE proteins in MICA an PVR up-regulation, we inhibited their
365 expression by using fomivirsen (also known as ISIS 2922), an antisense oligodeoxynucleotide
366 complementary to IE2 mRNA, and able to prevent both IE1 and IE2 protein expression when used at
367 certain concentration (44,45). This approach allowed us to specifically address the role of IE proteins in
368 regulating ligand expression within the context of HCMV infection. To this end, HFFs were treated with
369 different doses of fomivirsen, from 1 h before and throughout the entire infection (Fig. 8). At the highest
370 dose of fomivirsen (500 nM), expression of both IE1 and IE2 was inhibited (Fig. 8C-D) as previously
371 observed by Azad et al. (44) and, as expected, MICA and PVR up-regulation could not be detected (Fig.
372 8A-B). By progressively decreasing the concentration of fomivirsen (to 5 and 1 nM), we could rescue
373 IE1 protein expression (which was the first IE protein to reappear), and IE2 (Fig. 8C-D). At these low
374 concentrations of fomivirsen, recovery in HCMV-induced ligand up-regulation was observed (Fig. 8A-
375 B).
376 These results clearly demonstrated that the specific inhibition of IE protein expression in the context of
377 HCMV infection prevented MICA and PVR increase, therefore supporting the importance of these viral
378 proteins in the HCMV-mediated ligand regulation.
379 Next, we further examined the possibility that IE proteins could activate *MICA* and *PVR* gene promoters.
380 Thus, we co-transfected HFFs with pGL3-*MICA* (58) or pGL2-*PVR* (60) luciferase reporter plasmids,
381 harboring respectively -1 kb and -571 bp *MICA* and *PVR* promoter regions, together with IE1 or IE2
382 expression vectors. We observed that only IE2 transactivated *MICA* promoter, up to ~3-fold compared to
383 the control. Transfection of IE1, alone or together with IE2, did not significantly affect *MICA* promoter
384 activity, compared to IE2 alone (Fig. 9A). These results are in line with previous observations obtained
385 on the regulation of MICA mRNA and cell surface expression in cells transduced with AdV IE2.

We then analyzed IE2 structural requirements and its interaction with *MICA* promoter sequences. Firstly, we observed that expression of IE55, which lacks the transcriptional activation and DNA binding properties of IE2, was a poor transactivator of *MICA*, either in combination with IE1 (Fig. 9B), or alone (Fig. 9D). Then, a zinc finger mutant of IE2, which cannot bind to DNA but retains the ability to transactivate E gene promoters by protein-protein interactions (61,64), did not significantly increase *MICA* promoter activity, neither with IE1, nor alone (Fig. 9C and E). These results indicate that the IE2 functional domains located primarily toward the C-terminal end of the protein are required to transactivate *MICA* gene promoter.

Then, we used a shorter *MICA* construct (*MICA* -270 bp) to map the region(s) targeted by IE proteins. This fragment was indeed activated by IE1 and IE2 at similar levels compared to the longer *MICA* -1 kb region, indicating that the IE-responsive region was contained within the 270 bp fragment (Fig. 10A).

IE2-binding sites identified on viral and cellular promoters contain invariant CG residues at both ends of a 10-nucleotide sequence (CG-N_{10}-CG) (20,25,65,66), and we found a similar sequence within *MICA* promoter, between residues –92 and –78 (Fig. 10B). To evaluate the contribution of this putative IE2-binding site to the overall IE2-dependent transactivation of *MICA*, we changed by site-directed mutagenesis this unique CG-N_{10}-CG motif into a AT-N_{10}-AT sequence within the context of the *MICA* -270 construct. The introduced mutations significantly reduced IE2-dependent transactivation of *MICA*, thus supporting an involvement of the putative IE2-binding site in the regulation of this promoter (Fig. 10A-B).

We then addressed the capability of IE1/IE2 proteins to directly bind to *MICA* promoter by ChIP assays, using the wild-type or the CG-mutant form of *MICA*, in highly transfectable 293T cells. Using an anti-IE antibody and specific primers to amplify the region containing the putative IE2 binding site, we observed that IE1/IE2 were recruited to *MICA* promoter. The interaction was not detectable with the empty vector pSG5 or using normal rabbit serum as a negative control (Fig. 10C). Disruption of the putative IE2-

binding site of *MICA* reduced IE binding of about ~60%, further demonstrating that this sequence is involved in the IE2-dependent transactivation of *MICA* (Fig. 10D). The binding was confirmed on the endogenous *MICA* promoter as well, and it was detectable only when IE2 was expressed (Fig. 10E).

Together, these results demonstrate the capability of IE2 to directly bind sequences within *MICA* gene promoter, and that this binding is required for *MICA* transcriptional activation.

In relation to PVR, we performed similar transient cotransfection assays with a PVR -571 bp construct (60) and vectors expressing IE proteins. Though IE1 activated *PVR* promoter up to 10-fold over the control, the combination of IE1 and IE2 induced a prominent transcriptional activation that exceeded significantly the effect of IE1 alone. IE2 was instead ineffective in stimulating *PVR* (Fig. 11A). In contrast to what observed for *MICA*, expression of IE55 and of IE2 zinc finger mutant did not affect *PVR* promoter activity (Fig. 11B-C). Finally, to identify the IE-responsive region(s), we cotransfected IE1 and IE2, alone or in combination, with progressive deletions of *PVR* promoter (Fig. 11D-E) (60), and observed a significant drop in luciferase activity with the truncated sequences between -281 and -213 bp, indicating that this fragment mediated most of the transactivating activity resulting from the combination of IE1 and IE2, and only in minor part from IE1 alone (Fig. 11E).

Taken together, the results of this section indicate that the increase in cell surface expression of MICA and PVR upon HCMV infection is mediated by IE proteins through the transcriptional activation of their gene promoters.

Discussion

The molecular mechanisms driving the expression of NKG2DL and DNAM-1L remain largely unknown, particularly in virus-infected cells. In this study, we investigated the impact of HCMV infection on their expression and showed that MICA, ULBP3 and PVR are up-regulated on infected cells, in different cell type-viral strain combinations. For MICA, data suggest that its increased or *de novo* expression may be restricted to certain cell types, as it was observed on infected fibroblasts independently from the strain used, but not in endothelial or epithelial cells. Information on a cell-type specific regulation of MICA expression are currently not available, and further investigations would be of unquestionable interest for a better characterization of this molecule. However, the evidence that in primary fibroblasts MICA was induced by both laboratory and low-passage HCMV strains suggests that the down-modulating activity exerted by the viral proteins UL142, US9, US18 and US20 on this ligand (14-17) was not sufficient to prevent its overall cell surface expression. Similarly, though UL142 was described to prevent expression of ULBP3 as well (67), in our settings this ligand was always increased, consistently with previous findings (57). These discrepancies may be related to different experimental conditions and/or to the considerable polymorphism in the UL142 sequence among different strains (68,69). Thus, some variants of viral proteins may be less efficient at down-modulating NKG2DLs than others. At the same time, polymorphisms in both the coding and non-coding regions of MICA and ULBP3 (70-73) may also impact their expression upon HCMV infection. Thus, a prediction deriving from the presence of NKG2DL on the cell surface of HCMV-infected targets would be that blocking the receptor in cytotoxicity assays results in a decreased NK cell lysis. Indeed, this was the outcome of blocking experiments (Fig. 3), which demonstrated that the NKG2D receptor plays a role in the elimination of infected cells, as previously shown (57).

In relation to PVR, at present there are few reports on its regulation by HCMV (74-76). In particular, its expression resulted down-modulated in fibroblasts infected with the low-passage strain Merlin (74,75). In

contrast, our results show for the first time that PVR can be up-regulated by HCMV infection, in different cell types and with different viral strains, thus offering the immune system the opportunity to detect and react against infected cells through the activating receptor DNAM-1. Indeed, blocking of DNAM-1 in killing assays resulted in a significant inhibition of target cell lysis, similarly to what we observed for NKG2D (Fig. 3). Thus, from a functional point of view, the numerous HCMV immunoevasion strategies evolved against NKG2D and DNAM-1 ligands seems to be not completely successful, since these activating receptors still play a role in eliminating infected cells, including those infected with low-passage strains, which are *per se* less susceptible to NK killing (this study and ref.(14,15,57,62). In line with our data, DNAM-1 plays a relevant role in NK cell recognition of HCMV-infected myeloid dendritic cells early in infection, whereas the effect of viral-mediated down-regulation of DNAM-1L prevails at later stages, thus underlying the importance of the kinetics of immune evasion mechanisms (76). Moreover, a recent study demonstrated that DNAM-1L are rapidly induced during murine CMV infection *in vivo*, and the engagement of DNAM-1 is essential for the optimal NK cell-mediated host defense against the virus (11). Of note, as DNAM-1 is also expressed by many other leukocyte subsets and is an important activator of their effector functions, it may impact on a wide range of immunological responses (8,12,13,77).

To gain insights into the molecular mechanisms regulating the expression of activating ligands in infected cells, we investigated the role of DDR, a host cell pathway that positively affects the expression of activating ligands (35-43), and that it is activated by HCMV (26,27,29-34). Nevertheless, in HCMV-infected HFFs, MICA, ULBP3, and PVR were still increased even if ATM, ATR, and/or DNA-PK were knocked-down, thus indicating that these DDR kinases are not involved in the HCMV-mediated ligand stimulation, similarly to what has been reported for murine NKG2DL during murine CMV infection (78). HCMV IE proteins have been suggested to be implicated in the regulation of MIC proteins (16,79), but the molecular mechanism(s) are unknown. Moreover, no data have been reported on the regulation of

PVR by HCMV. Our results show that ectopic expression of IE1 and IE2 induced a significant increase of MICA and PVR, both at the mRNA and cell surface level. In particular, IE2 emerged as the main transactivator of *MICA* promoter, with the effect strictly dependent on its DNA binding activity, since it was lost in the presence of the IE55 isoform or the zinc finger mutant form of IE2. Accordingly, through ChIP and mutagenesis approaches, we identified an IE2 consensus sequence within the *MICA* gene promoter that turned out to be critical for *MICA* promoter transactivation by IE2.

This observation contributes to challenge the prevailing view that activation of cellular genes by IE2 depends from interactions with basal transcription factors, while nucleotide-specific binding of IE2 is the predominant mode of regulation of HCMV promoters (19-21,25,65). Moreover, this finding also suggests that the IE2-binding sites on cellular versus HCMV promoters are different, with the 10-internal nucleotides of the CG-N_{10}-CG motifs being GC-rich, rather than AT-rich, as previously suggested for the *cyclin E* promoter (66), and support the idea that IE2 is relatively sequence tolerant (25,65,66).

In regard to PVR, our results demonstrate a different mechanism of the HCMV-induced up-regulation. In fact, PVR mRNA and protein up-regulation required the co-expression of both IE1 and IE2. Furthermore, by using progressive deletions of *PVR* promoter, we mapped a region between -281 bp and -213 bp mostly responsive to IE1/IE2 combination. This fragment contains a potential IE2-responsive CG-N_{10}-CG element (from -271 to -257: CG-CAGGCGCAGG-CG), but it is unlikely that IE1/IE2 proteins bind to *PVR* promoter since the IE55 isoform and the zinc finger mutant of IE2 retained the capability to activate *PVR* promoter, and IE1 seems not to bind DNA directly (18). Accordingly, in ChIP assays we were unable to observe any detectable binding to the *PVR* promoter neither of the single IE proteins, nor of their combination (data not shown). Thus, it is more likely that the -281/-213 bp region contains the binding site(s) of cellular transcription factor(s) recruited and/or activated by IE proteins. In fact, this 68 bp region contains putative binding sites for several transcription factors, such as E2F, Sp1, AP-2α, Nrf-

1, and NF-kB (Fionda et al., unpublished observations), but further studies should be undertaken to identify which are the cellular proteins involved in the IE-mediated activation of *PVR* promoter.

As a final consideration on the importance of IE proteins in the regulation of MICA and PVR gene expression, we should also underline that it was observed not only by IE overexpression, but also in the context of HCMV infection. Indeed, by using fomivirsen (44,45), we observed that the inhibition of IE protein expression prevented the HCMV-induced MICA and PVR up-regulation (Fig. 8). Conversely, regaining IE protein expression by lower doses of fomivirsen, resulted in a recovery of ligand upregulation as well. These data thus clearly demonstrate that inhibition of IE protein expression in HCMV-infected cells prevents MICA and PVR increase.

In regard to ULBP3 regulation, though we could detect a significant increase in its mRNA and cell surface level upon HMCV infection, overexpressing IE1/IE2 by adenoviral vectors did not have a major effect on the expression of this ligand (Fig. S4), suggesting that IE1/IE2 were not sufficient for ULBP3 up-regulation.

From our study, two questions arise: the first one is why a virus should increase the expression of molecules involved in the elimination of infected cells? A possible answer could derive from the absolute requirement of IE proteins for a productive viral replication (18,19), with the induction of NKG2DL and DNAM-1L being an unavoidable side effect of the strong transactivating activity of IE2. In this scenario, up-regulation of activating ligands in HCMV-infected cells may represent an acceptable toll to pay to survive. Moreover, the IE2-consensus sequence we identified is conserved among different allelic variants of *MICA* promoter (Fionda et al., unpublished observations, and ref. (72,73), suggesting that during the virus-host co-evolution, a positive selection of promoter sequences in *MICA* alleles carrying the IE2 DNA binding site occurred, with the host likely making IE2 useful for its own cellular gene expression as well. The second question is how can we reconcile the observed HMCV-triggered increase of activating ligands with the immunoevasion strategies evolved by the virus to target the same

molecules? There could be a *window of opportunity*, a temporal frame in the early phases of HMCV infection, during which the unavoidable up-regulation of NKG2DL and DNAM-1L by IE proteins precedes the late expression of virus-encoded immunoevasion proteins. Thus, with elevated, functionally relevant levels of activating signals, the immune surveillance against the viral infection could be sufficiently robust, allowing recognition of infected cells by cytotoxic lymphocytes even at early times of infection. Moreover, HMCV diversity and tropism could have an important role as well. In fact, a hallmark of HCMV infections is its dissemination to a wide range of host tissues and cell types (3) with significant differences in the level of virus diversity between different compartments (80,81). Although it is not yet clear neither the mechanism explaining HCMV compartmentalization and intrahost genetic diversity, nor their effects on clinical disease, one possibility is that the generation of mutants may influence NK cell and/or T cell recognition, depending on the compartment (81).

In conclusion, our findings contribute to improve the understanding of the mechanisms underlying the regulation of the expression of NKG2D and DNAM-1 ligands, and consequently affecting immune responses mediated by their activating receptors expressed on all cytotoxic lymphocytes. This knowledge may be exploited to take full advantage of this potent immune pathway for therapeutic purposes.

Acknowledgements

We wish to thank Jay A. Nelson, Tim Kowalik, Marco Colonna, Jack D. Bui, Günter Bernhardt, Giuseppe Gerna, Andrea Gallina and Maurizio Fanciulli for reagents; members of the Santoni laboratory for discussions, and John Hiscott for a critical reading of the manuscript.

References

1. Britt, W. 2008. Manifestations of human cytomegalovirus infection: proposed mechanisms of acute and chronic disease. *Curr. Top. Microbiol. Immunol.* 325: 417-470.
2. Mocarski, E. S., T. Shenk, P. Griffiths, and Pass R.F. 2013. Citomegaloviruses. In *Fields Virology*, sixth ed. Knipe D.M. and Howley P.M., eds. Lippincott Williams & Wilkins, Philadelphia. 1960-2014.
3. Sinzger, C., M. Digel, and G. Jahn. 2008. Cytomegalovirus cell tropism. *Curr. Top. Microbiol. Immunol.* 325: 63-83.
4. Boeckh, M., W. J. Murphy, and K. S. Peggs. 2015. Recent advances in cytomegalovirus: an update on pharmacologic and cellular therapies. *Biol. Blood Marrow Transplant.* 21: 24-29.
5. Chou, S. 2015. Approach to drug-resistant cytomegalovirus in transplant recipients. *Curr. Opin. Infect. Dis.* 28: 293-299.
6. Eagle, R. A., and J. Trowsdale. 2007. Promiscuity and the single receptor: NKG2D. *Nat. Rev. Immunol.* 7: 737-744.
7. Champsaur, M., and L. L. Lanier. 2010. Effect of NKG2D ligand expression on host immune responses. *Immunol. Rev.* 235: 267-285.
8. Fuchs, A., and M. Colonna. 2006. The role of NK cell recognition of nectin and nectin-like proteins in tumor immunosurveillance. *Semin. Cancer Biol.* 16: 359-366.
9. Cella, M., R. Presti, W. Vermi, K. Lavender, E. Turnbull, C. Ochsenbauer-Jambor, J. C. Kappes, G. Ferrari, L. Kessels, I. Williams, A. J. McMichael, B. F. Haynes, P. Borrow, and M. Colonna. 2010. Loss of DNAM-1 contributes to CD8+ T-cell exhaustion in chronic HIV-1 infection. *Eur. J. Immunol.* 40: 949-954.
10. Welch, M. J., J. R. Teijaro, H. A. Lewicki, M. Colonna, and M. B. Oldstone. 2012. CD8 T cell defect of TNF-alpha and IL-2 in DNAM-1 deficient mice delays clearance in vivo of a persistent virus infection. *Virology* 429: 163-170.
11. Nabekura, T., M. Kanaya, A. Shibuya, G. Fu, N. R. Gascoigne, and L. L. Lanier. 2014. Costimulatory molecule DNAM-1 is essential for optimal differentiation of memory natural killer cells during mouse cytomegalovirus infection. *Immunity.* 40: 225-234.
12. de Andrade, L. F., M. J. Smyth, and L. Martinet. 2014. DNAM-1 control of natural killer cells functions through nectin and nectin-like proteins. *Immunol. Cell Biol.* 92: 237-244.

13. Takai, Y., J. Miyoshi, W. Ikeda, and H. Ogita. 2008. Nectins and nectin-like molecules: roles in contact inhibition of cell movement and proliferation. *Nat. Rev. Mol. Cell Biol.* 9: 603-615.
14. Wilkinson, G. W., P. Tomasec, R. J. Stanton, M. Armstrong, V. Prod'homme, R. Aicheler, B. P. McSharry, C. R. Rickards, D. Cochrane, S. Llewellyn-Lacey, E. C. Wang, C. A. Griffin, and A. J. Davison. 2008. Modulation of natural killer cells by human cytomegalovirus. *J. Clin. Virol.* 41: 206-212.
15. Rossini, G., C. Cerboni, A. Santoni, M. P. Landini, S. Landolfo, D. Gatti, G. Gribaudo, and S. Varani. 2012. Interplay between human cytomegalovirus and intrinsic/innate host responses: a complex bidirectional relationship. *Mediators. Inflamm.* 2012: 607276.
16. Fielding, C. A., R. Aicheler, R. J. Stanton, E. C. Wang, S. Han, S. Seirafian, J. Davies, B. P. McSharry, M. P. Weekes, P. R. Antrobus, V. Prod'homme, F. P. Blanchet, D. Sugrue, S. Cuff, D. Roberts, A. J. Davison, P. J. Lehner, G. W. Wilkinson, and P. Tomasec. 2014. Two novel human cytomegalovirus NK cell evasion functions target MICA for lysosomal degradation. *PLoS. Pathog.* 10: e1004058.
17. Seidel, E., V. T. Le, Y. Bar-On, P. Tsukerman, J. Enk, R. Yamin, N. Stein, D. Schmiedel, D. E. Oiknine, Y. Weisblum, B. Tirosh, P. Stastny, D. G. Wolf, H. Hengel, and O. Mandelboim. 2015. Dynamic Co-evolution of Host and Pathogen: HCMV Downregulates the Prevalent Allele MICA *008 to Escape Elimination by NK Cells. *Cell Rep.* 10: 968-982.
18. Castillo, J. P., and T. F. Kowalik. 2002. Human cytomegalovirus immediate early proteins and cell growth control. *Gene* 290: 19-34.
19. Stinski, M. F., and D. T. Petrik. 2008. Functional roles of the human cytomegalovirus essential IE86 protein. *Curr. Top. Microbiol. Immunol.* 325: 133-152.
20. Lang, D., and T. Stamminger. 1993. The 86-kilodalton IE-2 protein of human cytomegalovirus is a sequence-specific DNA-binding protein that interacts directly with the negative autoregulatory response element located near the cap site of the IE-1/2 enhancer-promoter. *J. Virol.* 67: 323-331.
21. Malone, C. L., D. H. Vesole, and M. F. Stinski. 1990. Transactivation of a human cytomegalovirus early promoter by gene products from the immediate-early gene IE2 and augmentation by IE1: mutational analysis of the viral proteins. *J. Virol.* 64: 1498-1506.
22. Pizzorno, M. C., M. A. Mullen, Y. N. Chang, and G. S. Hayward. 1991. The functionally active IE2 immediate-early regulatory protein of human cytomegalovirus is an 80-kilodalton polypeptide

that contains two distinct activator domains and a duplicated nuclear localization signal. *J. Virol.* 65: 3839-3852.

23. Chiou, C. J., J. Zong, I. Waheed, and G. S. Hayward. 1993. Identification and mapping of dimerization and DNA-binding domains in the C terminus of the IE2 regulatory protein of human cytomegalovirus. *J. Virol.* 67: 6201-6214.
24. Klucher, K. M., M. Sommer, J. T. Kadonaga, and D. H. Spector. 1993. In vivo and in vitro analysis of transcriptional activation mediated by the human cytomegalovirus major immediate-early proteins. *Mol. Cell Biol.* 13: 1238-1250.
25. Schwartz, R., M. H. Sommer, A. Scully, and D. H. Spector. 1994. Site-specific binding of the human cytomegalovirus IE2 86-kilodalton protein to an early gene promoter. *J. Virol.* 68: 5613-5622.
26. Castillo, J. P., F. M. Frame, H. A. Rogoff, M. T. Pickering, A. D. Yurochko, and T. F. Kowalik. 2005. Human cytomegalovirus IE1-72 activates ataxia telangiectasia mutated kinase and a p53/p21-mediated growth arrest response. *J. Virol.* 79: 11467-11475.
27. Xiaofei E, M. T. Pickering, M. Debatis, J. Castillo, A. Lagadinos, S. Wang, S. Lu, and T. F. Kowalik. 2011. An E2F1-mediated DNA damage response contributes to the replication of human cytomegalovirus. *PLoS. Pathog.* 7: e1001342.
28. Jackson, S. P., and J. Bartek. 2009. The DNA-damage response in human biology and disease. *Nature* 461: 1071-1078.
29. Shen, Y. H., B. Utama, J. Wang, M. Raveendran, D. Senthil, W. J. Waldman, J. D. Belcher, G. Vercellotti, D. Martin, B. M. Mitchelle, and X. L. Wang. 2004. Human cytomegalovirus causes endothelial injury through the ataxia telangiectasia mutant and p53 DNA damage signaling pathways. *Circ. Res.* 94: 1310-1317.
30. Gaspar, M., and T. Shenk. 2006. Human cytomegalovirus inhibits a DNA damage response by mislocalizing checkpoint proteins. *Proc. Natl. Acad. Sci. U. S. A* 103: 2821-2826.
31. Luo, M. H., K. Rosenke, K. Czornak, and E. A. Fortunato. 2007. Human cytomegalovirus disrupts both ataxia telangiectasia mutated protein (ATM)- and ATM-Rad3-related kinase-mediated DNA damage responses during lytic infection. *J. Virol.* 81: 1934-1950.
32. Li, R., J. Zhu, Z. Xie, G. Liao, J. Liu, M. R. Chen, S. Hu, C. Woodard, J. Lin, S. D. Taverna, P. Desai, R. F. Ambinder, G. S. Hayward, J. Qian, H. Zhu, and S. D. Hayward. 2011. Conserved

herpesvirus kinases target the DNA damage response pathway and TIP60 histone acetyltransferase to promote virus replication. *Cell Host. Microbe* 10: 390-400.

33. Xiaofei E, G. Savidis, C. R. Chin, S. Wang, S. Lu, A. L. Brass, and T. F. Kowalik. 2014. A novel DDB2-ATM feedback loop regulates human cytomegalovirus replication. *J. Virol.* 88: 2279-2290.
34. Xiaofei, E., and T. F. Kowalik. 2014. The DNA damage response induced by infection with human cytomegalovirus and other viruses. *Viruses.* 6: 2155-2185.
35. Gasser, S., S. Orsulic, E. J. Brown, and D. H. Raulet. 2005. The DNA damage pathway regulates innate immune system ligands of the NKG2D receptor. *Nature* 436: 1186-1190.
36. Cerboni, C., A. Zingoni, M. Cippitelli, M. Piccoli, L. Frati, and A. Santoni. 2007. Antigen-activated human T lymphocytes express cell-surface NKG2D ligands via an ATM/ATR-dependent mechanism and become susceptible to autologous NK- cell lysis. *Blood* 110: 606-615.
37. Soriani, A., A. Zingoni, C. Cerboni, M. L. Iannitto, M. R. Ricciardi, G. Di, V, M. Cippitelli, C. Fionda, M. T. Petrucci, A. Guarini, R. Foa, and A. Santoni. 2009. ATM-ATR-dependent up-regulation of DNAM-1 and NKG2D ligands on multiple myeloma cells by therapeutic agents results in enhanced NK-cell susceptibility and is associated with a senescent phenotype. *Blood* 113: 3503-3511.
38. Ardolino, M., A. Zingoni, C. Cerboni, F. Cecere, A. Soriani, M. L. Iannitto, and A. Santoni. 2011. DNAM-1 ligand expression on Ag-stimulated T lymphocytes is mediated by ROS-dependent activation of DNA-damage response: relevance for NK-T cell interaction. *Blood* 117: 4778-4786.
39. Cerboni, C., C. Fionda, A. Soriani, A. Zingoni, M. Doria, M. Cippitelli, and A. Santoni. 2014. The DNA Damage Response: A Common Pathway in the Regulation of NKG2D and DNAM-1 Ligand Expression in Normal, Infected, and Cancer Cells. *Front Immunol.* 4: 508.
40. Fionda, C., M. P. Abruzzese, A. Zingoni, A. Soriani, B. Ricci, R. Molfetta, R. Paolini, A. Santoni, and M. Cippitelli. 2015. Nitric oxide donors increase PVR/CD155 DNAM-1 ligand expression in multiple myeloma cells: role of DNA damage response activation. *BMC. Cancer* 15: 17.
41. Ward, J., Z. Davis, J. DeHart, E. Zimmerman, A. Bosque, E. Brunetta, D. Mavilio, V. Planelles, and E. Barker. 2009. HIV-1 Vpr triggers natural killer cell-mediated lysis of infected cells through activation of the ATR-mediated DNA damage response. *PLoS. Pathog.* 5: e1000613.
42. Richard, J., S. Sindhu, T. N. Pham, J. P. Belzile, and E. A. Cohen. 2010. HIV-1 Vpr up-regulates expression of ligands for the activating NKG2D receptor and promotes NK cell-mediated killing. *Blood* 115: 1354-1363.

43. Vassena, L., E. Giuliani, G. Matusali, E. A. Cohen, and M. Doria. 2013. The human immunodeficiency virus type 1 Vpr protein upregulates PVR via activation of the ATR-mediated DNA damage response pathway. *J. Gen. Virol.* 94: 2664-2669.
44. Azad, R. F., V. B. Driver, K. Tanaka, R. M. Crooke, and K. P. Anderson. 1993. Antiviral activity of a phosphorothioate oligonucleotide complementary to RNA of the human cytomegalovirus major immediate-early region. *Antimicrob. Agents Chemother.* 37: 1945-1954.
45. Luganini, A., P. Caposio, M. Mondini, S. Landolfo, and G. Gribaudo. 2008. New cell-based indicator assays for the detection of human cytomegalovirus infection and screening of inhibitors of viral immediate-early 2 protein activity. *J. Appl. Microbiol.* 105: 1791-1801.
46. Bruno, T., N. F. De, S. Iezzi, D. Lecis, C. D'Angelo, P. M. Di, N. Corbi, L. Dimiziani, L. Zannini, C. Jekimovs, M. Scarsella, A. Porrello, A. Chersi, M. Crescenzi, C. Leonetti, K. K. Khanna, S. Soddu, A. Floridi, C. Passananti, D. Delia, and M. Fanciulli. 2006. Che-1 phosphorylation by ATM/ATR and Chk2 kinases activates p53 transcription and the G2/M checkpoint. *Cancer Cell* 10: 473-486.
47. Smith, I. L., I. Taskintuna, F. M. Rahhal, H. C. Powell, E. Ai, A. J. Mueller, S. A. Spector, and W. R. Freeman. 1998. Clinical failure of CMV retinitis with intravitreal cidofovir is associated with antiviral resistance. *Arch. Ophthalmol.* 116: 178-185.
48. Murphy, E., D. Yu, J. Grimwood, J. Schmutz, M. Dickson, M. A. Jarvis, G. Hahn, J. A. Nelson, R. M. Myers, and T. E. Shenk. 2003. Coding potential of laboratory and clinical strains of human cytomegalovirus. *Proc. Natl. Acad. Sci. U. S. A* 100: 14976-14981.
49. Ryckman, B. J., M. A. Jarvis, D. D. Drummond, J. A. Nelson, and D. C. Johnson. 2006. Human cytomegalovirus entry into epithelial and endothelial cells depends on genes UL128 to UL150 and occurs by endocytosis and low-pH fusion. *J. Virol.* 80: 710-722.
50. Bronzini, M., A. Luganini, V. Dell'Oste, A. M. De, S. Landolfo, and G. Gribaudo. 2012. The US16 gene of human cytomegalovirus is required for efficient viral infection of endothelial and epithelial cells. *J. Virol.* 86: 6875-6888.
51. Grazia, R. M., F. Baldanti, E. Percivalle, A. Sarasini, L. De-Giuli, E. Genini, D. Lilleri, N. Labo, and G. Gerna. 2001. In vitro selection of human cytomegalovirus variants unable to transfer virus and virus products from infected cells to polymorphonuclear leukocytes and to grow in endothelial cells. *J. Gen. Virol.* 82: 1429-1438.

52. Caposio, P., T. Musso, A. Luganini, H. Inoue, M. Gariglio, S. Landolfo, and G. Gribaudo. 2007. Targeting the NF-kappaB pathway through pharmacological inhibition of IKK2 prevents human cytomegalovirus replication and virus-induced inflammatory response in infected endothelial cells. *Antiviral Res.* 73: 175-184.
53. Sarkaria, J. N., E. C. Busby, R. S. Tibbetts, P. Roos, Y. Taya, L. M. Karnitz, and R. T. Abraham. 1999. Inhibition of ATM and ATR kinase activities by the radiosensitizing agent, caffeine. *Cancer Res.* 59: 4375-4382.
54. Block, W. D., D. Merkle, K. Meek, and S. P. Lees-Miller. 2004. Selective inhibition of the DNA-dependent protein kinase (DNA-PK) by the radiosensitizing agent caffeine. *Nucleic Acids Res.* 32: 1967-1972.
55. Gariano, G. R., V. Dell'Oste, M. Bronzini, D. Gatti, A. Luganini, A. M. De, G. Gribaudo, M. Gariglio, and S. Landolfo. 2012. The intracellular DNA sensor IFI16 gene acts as restriction factor for human cytomegalovirus replication. *PLoS. Pathog.* 8: e1002498.
56. Mercorelli, B., A. Luganini, G. Muratore, S. Massari, M. E. Terlizzi, O. Tabarrini, G. Gribaudo, G. Palu, and A. Loregian. 2014. The 6-Aminoquinolone WC5 inhibits different functions of the immediate-early 2 (IE2) protein of human cytomegalovirus that are essential for viral replication. *Antimicrob. Agents Chemother.* 58: 6615-6626.
57. Rolle, A., M. Mousavi-Jazi, M. Eriksson, J. Odeberg, C. Soderberg-Naucler, D. Cosman, K. Karre, and C. Cerboni. 2003. Effects of human cytomegalovirus infection on ligands for the activating NKG2D receptor of NK cells: up-regulation of UL16-binding protein (ULBP)1 and ULBP2 is counteracted by the viral UL16 protein. *J. Immunol.* 171: 902-908.
58. Yadav, D., J. Ngolab, R. S. Lim, S. Krishnamurthy, and J. D. Bui. 2009. Cutting edge: down-regulation of MHC class I-related chain A on tumor cells by IFN-gamma-induced microRNA. *J. Immunol.* 182: 39-43.
59. Soriani, A., M. L. Iannitto, B. Ricci, C. Fionda, G. Malgarini, S. Morrone, G. Peruzzi, M. R. Ricciardi, M. T. Petrucci, M. Cippitelli, and A. Santoni. 2014. Reactive oxygen species- and DNA damage response-dependent NK cell activating ligand upregulation occurs at transcriptional levels and requires the transcriptional factor E2F1. *J. Immunol.* 193: 950-960.
60. Solecki, D., S. Schwarz, E. Wimmer, M. Lipp, and G. Bernhardt. 1997. The promoters for human and monkey poliovirus receptors. Requirements for basic and cell type-specific activity. *J. Biol. Chem.* 272: 5579-5586.

61. Jupp, R., S. Hoffmann, A. Depto, R. M. Stenberg, P. Ghazal, and J. A. Nelson. 1993. Direct interaction of the human cytomegalovirus IE86 protein with the cis repression signal does not preclude TBP from binding to the TATA box. *J. Virol.* 67: 5595-5604.
62. Cerboni, C., M. Mousavi-Jazi, A. Linde, K. Soderstrom, M. Brytting, B. Wahren, K. Karre, and E. Carbone. 2000. Human cytomegalovirus strain-dependent changes in NK cell recognition of infected fibroblasts. *J. Immunol.* 164: 4775-4782.
63. Tyms, A. S., J. M. Davis, J. R. Clarke, and D. J. Jeffries. 1987. Synthesis of cytomegalovirus DNA is an antiviral target late in virus growth. *J. Gen. Virol.* 68): 1563-1573.
64. Jupp, R., S. Hoffmann, R. M. Stenberg, J. A. Nelson, and P. Ghazal. 1993. Human cytomegalovirus IE86 protein interacts with promoter-bound TATA-binding protein via a specific region distinct from the autorepression domain. *J. Virol.* 67: 7539-7546.
65. Arlt, H., D. Lang, S. Gebert, and T. Stamminger. 1994. Identification of binding sites for the 86-kilodalton IE2 protein of human cytomegalovirus within an IE2-responsive viral early promoter. *J. Virol.* 68: 4117-4125.
66. Bresnahan, W. A., T. Albrecht, and E. A. Thompson. 1998. The cyclin E promoter is activated by human cytomegalovirus 86-kDa immediate early protein. *J. Biol. Chem.* 273: 22075-22082.
67. Bennett, N. J., O. Ashiru, F. J. Morgan, Y. Pang, G. Okecha, R. A. Eagle, J. Trowsdale, J. G. Sissons, and M. R. Wills. 2010. Intracellular sequestration of the NKG2D ligand ULBP3 by human cytomegalovirus. *J. Immunol.* 185: 1093-1102.
68. Chalupny, N. J., A. Rein-Weston, S. Dosch, and D. Cosman. 2006. Down-regulation of the NKG2D ligand MICA by the human cytomegalovirus glycoprotein UL142. *Biochem. Biophys. Res. Commun.* 346: 175-181.
69. Wilkinson, G. W., A. J. Davison, P. Tomasec, C. A. Fielding, R. Aicheler, I. Murrell, S. Seirafian, E. C. Wang, M. Weekes, P. J. Lehner, G. S. Wilkie, and R. J. Stanton. 2015. Human cytomegalovirus: taking the strain. *Med. Microbiol. Immunol.* 204: 273-284.
70. Eagle, R. A., J. A. Traherne, O. Ashiru, M. R. Wills, and J. Trowsdale. 2006. Regulation of NKG2D ligand gene expression. *Hum. Immunol.* 67: 159-169.
71. Choy, M. K., and M. E. Phipps. 2010. MICA polymorphism: biology and importance in immunity and disease. *Trends Mol. Med.* 16: 97-106.
72. Cox, S. T., J. A. Madrigal, and A. Saudemont. 2014. Diversity and characterization of polymorphic 5' promoter haplotypes of MICA and MICB genes. *Tissue Antigens* 84: 293-303.

73. Luo, J., W. Tian, F. Pan, X. Liu, and L. Li. 2014. Allelic and haplotypic diversity of 5'promoter region of the MICA gene. *Hum. Immunol.* 75: 383-388.
74. Tomasec, P., E. C. Wang, A. J. Davison, B. Vojtesek, M. Armstrong, C. Griffin, B. P. McSharry, R. J. Morris, S. Llewellyn-Lacey, C. Rickards, A. Nomoto, C. Sinzger, and G. W. Wilkinson. 2005. Downregulation of natural killer cell-activating ligand CD155 by human cytomegalovirus UL141. *Nat. Immunol.* 6: 181-188.
75. Prod'homme, V., D. M. Sugrue, R. J. Stanton, A. Nomoto, J. Davies, C. R. Rickards, D. Cochrane, M. Moore, G. W. Wilkinson, and P. Tomasec. 2010. Human cytomegalovirus UL141 promotes efficient downregulation of the natural killer cell activating ligand CD112. *J. Gen. Virol.* 91: 2034-2039.
76. Magri, G., A. Muntasell, N. Romo, A. Saez-Borderias, D. Pende, D. E. Geraghty, H. Hengel, A. Angulo, A. Moretta, and M. Lopez-Botet. 2011. NKp46 and DNAM-1 NK-cell receptors drive the response to human cytomegalovirus-infected myeloid dendritic cells overcoming viral immune evasion strategies. *Blood* 117: 848-856.
77. Martinet, L., A. L. Ferrari de, C. Guillerey, J. S. Lee, J. Liu, F. Souza-Fonseca-Guimaraes, D. S. Hutchinson, T. B. Kolesnik, S. E. Nicholson, N. D. Huntington, and M. J. Smyth. 2015. DNAM-1 expression marks an alternative program of NK cell maturation. *Cell Rep.* 11: 85-97.
78. Tokuyama, M., C. Lorin, F. Delebecque, H. Jung, D. H. Raulet, and L. Coscoy. 2011. Expression of the RAE-1 family of stimulatory NK-cell ligands requires activation of the PI3K pathway during viral infection and transformation. *PLoS. Pathog.* 7: e1002265.
79. Venkataraman, G. M., D. Suciu, V. Groh, J. M. Boss, and T. Spies. 2007. Promoter region architecture and transcriptional regulation of the genes for the MHC class I-related chain A and B ligands of NKG2D. *J. Immunol.* 178: 961-969.
80. Sowmya, P., and H. N. Madhavan. 2009. Analysis of mixed infections by multiple genotypes of human cytomegalovirus in immunocompromised patients. *J. Med. Virol.* 81: 861-869.
81. Renzette, N., L. Gibson, J. D. Jensen, and T. F. Kowalik. 2014. Human cytomegalovirus intrahost evolution-a new avenue for understanding and controlling herpesvirus infections. *Curr. Opin. Virol.* 8: 109-115.

Footnotes

This work was funded by grants from the Pasteur Institute-Cenci-Bolognetti Foundation, "Sapienza" University of Rome, Center of Excellence for Biology and Molecular Medicine (BEMM), Italian Ministry of Instruction, University and Research (MIUR) (Projects PRIN 2011, PRIN 2012, and PON), and the Medintech Cluster.

Abbreviations:

AdV, adenoviral vector; APC, allophycocyanin; ATM, ataxia-telangiectasia mutated; ATR, ataxia telangiectasia and Rad3-related protein; ChIP, chromatin immunoprecipitation; DDR, DNA damage response; DNAM-1L, DNAM-1 ligands; DNA-PK, DNA-dependent protein kinase; dpi, days post-infection; GAM, goat anti-mouse; γH2AX, phospho-histone H2AX; HCMV, human CMV; HFFs, human foreskin fibroblasts; HMVEC, human microvascular endothelial cells; IE, immediate early; E, early; L, late; MFI, mean of fluorescence intensity; MICA/B, MHC class I–related chain A/B; MIEP, major immediate early promoter; MOI, multiplicity of infection; NKG2DL, NKG2D ligands; PFA, phosphonoformic acid; PVR, poliovirus receptor; ULBP, UL16-binding protein.

Figure legends

Figure 1. NKG2D and DNAM-1 ligand expression on AD169-infected fibroblasts. HFFs were infected with HCMV AD169 (MOI 1 PFU/cell) or mock-infected (n.i.) and harvested at different days post-infection (dpi). Ligand expression was evaluated by FACS. **A)** A representative experiment of at least four performed at 3 dpi is shown. Dashed lines indicate isotypic control IgG on n.i. or infected cells. **B)** The kinetics of ligands with an increased expression upon HCMV infection is shown. Expression levels are presented as mean of fluorescence intensity (MFI). Data from at least four independent experiments ± SEs.

Figure 2. NKG2D and DNAM-1 ligands are up-regulated on different cell types by HCMV low-passage strains VR-1814 and TR. HFFs, HMVEC or ARPE-19 cells were mock-infected (n.i.) or infected with the indicated HCMV low-passage strain, and harvested at 3 dpi. **A)** A representative experiment of HFFs infected with the low-passage strain VR-1814, and with AD169 as a control, is shown. **B)** HFFs were infected with VR-1814 (MOI 1 and 5 PFU/cell). Data from three experiments ± SEs. **C)** HFFs, HMVEC, and ARPE-19 cells were infected with TR or VR-1814 (MOI 1 PFU/cell). Data from three or five (HFFs with TR) experiments ± SEs. Expression levels are presented as MFI.

Figure 3. Contribution of NKG2D and DNAM-1 to NK cell-mediated cytotoxicity against mock-infected (n.i.), AD169- or TR-infected HFFs (MOI 1, 3 dpi). **A)** A representative 4 h chromium-release assay in which effector cells were left untreated (no Ab), or were preincubated with anti-NKG2D, anti-DNAM-1, or IgG_1 isotype control mAb, is shown. **B)** Reduction of NK cell-mediated killing of n.i., AD169- or TR-infected HFFs by mAb treatment (pooled data from four experiments with NK cells obtained from different donors, at 50:1). Mean inhibition of lysis (%) was calculated in comparison to untreated NK

cells (no Ab), and statistical analysis was performed with ANOVA, as described in *Materials and Methods*.

Figure 4. Triple silencing of ATM, ATR and DNA-PK does not affect MICA, ULBP3 and PVR expression. HFFs were firstly transfected with DNA-PK siRNA or with a non-targeting siRNA (siCtrl). 24 h later, the same cells were co-transfected with ATM and ATR siRNA, or with siCtrl. Then, 24 h later, cells were either mock-infected (n.i.) or infected with AD169 (MOI 1 PFU/cell); then, at 3 dpi cells and supernatants were harvested. **A)** FACS of MICA, ULBP3 and PVR expression, derived from three experiments, with expression levels presented as MFI ± SEs. **B)** The % of IE+ cells was analyzed by FACS on HCMV-infected cells stained intracellularly with a specific anti-IE mAb. **C)** Cell culture supernatants were assayed for infectious virus production by plaque assay. **D)** Levels of ATM, ATR and DNA-PK protein expression were assayed by immunoblot analysis with specific antibodies. The p85 subunit of PI-3K was used as loading control. One representative experiment out of three is shown. **E)** The amounts of ATM, ATR and DNA-PK, normalized to that of p85, were determined by densitometric analysis and are relative to that in n.i./siRNA Ctrl cells, which was arbitrarily set as 1. Data are expressed as mean ± SEs of three independent experiments. ns: not statistically significant difference. siDDR: cells transfected with siATM, siATR and siDNA-PK.

Figure 5. Immediate early and early genes, but not late genes, are *per se* sufficient to increase the expression of MICA, ULBP3 and PVR in infected cells. HFFs were infected with HCMV AD169 (MOI 1 PFU/cell) or mock-infected (n.i.), and then treated with 200 µg/ml of phoshonoformic acid (PFA) immediately after infection. At 3 dpi, cells were harvested and stained for MICA, ULBP3, PVR or isotype control IgG, followed by GAM-FITC. Top panels: one representative experiment out of four is shown. Bottom panels: data are represented as MFI ± SEs of four independent experiments.

853

854 **Figure 6. Up-regulation of MICA, ULBP3 and PVR mRNA in HCMV-infected cells.** HFFs were
855 infected with HCMV AD169 (MOI 1 PFU/cell) or mock-infected (n.i.). At the indicated times post-
856 infection, total RNA was isolated and reverse transcribed. cDNAs were amplified by real-time PCR using
857 primers specific for MICA, ULBP3, PVR, or GAPDH. Data from four experiments, expressed as fold
858 change units ± SEs, were normalized with GAPDH and referred to n.i. cells considered as calibrators, and
859 set at 1.

860

861 **Figure 7. Adenoviral-mediated overexpression of IE1 and IE2 proteins increases mRNA and cell**
862 **surface expression of MICA and PVR.** HFFs were transduced with adenoviral vectors (AdV)
863 expressing IE1, IE2, or LacZ as a control, alone or in combination (total MOI 4 PFU/cell). Cells were
864 harvested 24 h, 48 h or 72 h later, and analyzed for ligand mRNA and surface expression. **A)** Real-time
865 PCR for MICA and PVR. Data from four experiments ± SEs, expressed as fold change units**,** were
866 normalized with GAPDH and referred to not-transduced cells (-), considered as calibrators and set at 1.
867 **B)** FACS of MICA and PVR expression, derived from three experiments at 72 hpi, with expression levels
868 presented as MFI ± SEs. **C)** MICA and PVR cell surface expression from a representative experiment
869 performed at 72 hpi. Statistical analysis was performed with ANOVA.

870

871 **Figure 8. MICA and PVR up-regulation during HCMV infection is inhibited in the presence of**
872 **fomivirsen.** HFFs were treated or not with the indicated dose of fomivirsen 1 h before, and then during
873 the infection with HCMV AD169 (MOI 1 PFU/cell). The drug was maintained in the culture medium
874 until cell harvesting and processing, at 3 dpi. **A, B)** FACS of MICA and PVR expression, derived from
875 four experiments, with expression levels presented as MFI ± SEs. **C)** Levels of IE1 and IE2 protein
876 expression were assayed by immunoblot analysis with anti-IE mAb. The p85 subunit of PI-3K was used

as loading control. One representative experiment out of four is shown. **D)** The amounts of IE proteins, normalized to that of p85, were determined by densitometric analysis and are relative to that in HCMV infected cells without fomivirsen, which was arbitrarily set as 1. Data are expressed as mean ± SEs of four independent experiments. Statistical analysis was performed with ANOVA.

Figure 9. IE2 activates *MICA* promoter: role of the DNA binding activity. A) HFFs were transfected with pGL3-MICA (-1 Kb fragment) luciferase reporter plasmid, together with IE1 and/or IE2 expression vectors, or with the empty control vector pSG5. After 48 h, transfected cells were harvested and protein extracts were used for luciferase assay. Luciferase activity was calculated as described in *Materials & Methods,* and results are expressed as fold-induction compared to pSG5. **B)** and **C)** IE2-86 was replaced by IE2-55 **(B)** or by a zinc finger domain mutant of IE2-86 (IE2-Zn mut) **(C)**. In panels **D)** and **E)** *MICA* promoter activation induced by IE2-55 **(D)** or IE2-Zn mut **(E)** alone is shown. Data from at least three experiments ± SEs.

Figure 10. Identification of an IE2 consensus site in *MICA* promoter. A) HFFs were transfected with wild-type (wt) pGL3-*MICA* (-270 bp fragment) promoter luciferase reporter vector, or with a mutated form (CG-mut), together with IE expression vectors, or pSG5. After 48 h, cells were harvested and luciferase activity was calculated as described in figure 9. Data from three experiments ± SEs. **B)** the CG-N_{10}-CG sequence identified on *MICA* promoter, and its mutated form (CG-mut), are reported and compared with some of the IE2-binding sites described on the HCMV MIEP, the 2.2 Kb early promoter and the *cyclin E* promoter. **C)** 293T cells were co-transfected with wt pGL3-*MICA* (-270 bp fragment) promoter, and IE expression vectors or pSG5. After 48 h, cells were harvested and processed for ChIP assays. Results are shown as relative enrichment of samples immunoprecipitated with the anti-IE antibody, respect to IgG control. Data from three experiments ± SEs. **D)** Both the wt and the mutant form

of -270 bp *MICA* promoter were used in ChIP experiments, and the relative enrichment compared. Data are expressed as percent of IE binding, with the relative enrichment of MICA -270 wt promoter set as 100%, and are from three experiments ± SEs. **E)** ChIP assays on the endogenous *MICA* promoter were performed by transfecting IE1, IE2 or pSG5 vectors. Results are reported as described in panel C), and are from three independent experiments ± SEs. MIEP: major immediate early promoter; CRS: *cis*-repression sequence.

Figure 11. Effect of IE1 and IE2 on the transcriptional activity of *PVR* gene promoter. A) HFFs were transfected with pGL2-PVR (-571 bp fragment) promoter luciferase reporter vector, together with IE expression vectors, used alone or in combination, or pSG5. After 48 h, cells were harvested and luciferase activity was calculated as reported in figure 9. **B, C)** IE2-86 was replaced by IE2-55 **(B)** or by a zinc finger domain mutant of IE2-86 (IE2-Zn mut) **(C),** as described in figure 9. **D)** HFFs were transiently transfected with wild-type pGL2-*PVR* (-571 bp fragment) promoter luciferase reporter vector, or with 5'-deletions constructs, together with IE expression vectors, or pSG5. After 48 h, cells were harvested and luciferase activity was calculated. Data from at least four experiments ± SEs. **E)** The effect of IE1 and IE2, alone or in combination, on PVR promoter deletions is shown. Data from at least four experiments ± SEs.

Supplementary Figure 1. HCMV AD169 and TR strains stimulate expression of cell surface MICA. HFFswere grown to subconfluence and then infected with HCMV AD169 and TR (MOI of 1 PFU/cell), or mock infected (n.i.). At 4 dpi, cells were fixed and immunostained for MICA ligand, without permeabilization. Immunofluorescence experiments were repeated three times, and representative results are presented. Magnification: 60X.

Supplementary Figure 2. Activation of DDR pathway after HCMV infection, and effect of the absence of

ATM on MICA, ULBP3 and PVR cell surface expression. A) HFFs were infected with HCMV AD169 (MOI of 1 PFU/cell) or mock-infected (n.i.) and harvested at 3 dpi. Phospho-histone H2AX (γH2AX) (Ser139) expression levels were evaluated by FACS on cells stained with a specific FITC-conjugated mAb. A representative experiment of four performed at 3 dpi is shown. B) Data are presented as fold induction of γH2AX MFI values in HCMV-infected versus n.i. cells, set at 1. Data from four experiments ± SEs. C) ATM-deficient (AT-/-) fibroblasts were mock-infected (n.i.) or infected with HCMV AD169 (MOI of 1 PFU/cell). At different dpi, cells were harvested and ligand expression was analyzed as in figure 1. A representative experiment out of three is shown. D-G) HFFs were transiently transfected with siRNA specific for ATM (siATM) or with a non-targeting siRNA (siCtrl). 24 h later, cells were either mock-infected (n.i.) or infected with HCMV AD169 (MOI of 1 PFU/cell). At 2 dpi, cells and supernatants were harvested and assayed for ligand expression, percentage of IE+ cells, infectious virus production, and immunoblot analysis. D) Flow cytometry analysis of MICA, ULBP3 and PVR expression was performed as described in figure 1. Vertical dotted lines indicate the center of the peak for each ligand in not infected-siCtrl transfected cells. All panels derive from the same experiment, representative of three. E) The % of IE+ cells was analyzed by FACS on HCMV-infected cells stained intracellularly with a specific anti-IE mAb. F). Cell culture supernatants were assayed for infectious virus production by plaque assay. G) The levels of ATM protein expression were assayed by immunoblot analysis with a specific antibody. Immunodetection of the p85 subunit of PI-3K was used as a control of protein loading. ns: not statistically significant difference with Student's t-test.

Supplementary Figure 3. ATR or DNA-PK silencing does not affect MICA, ULBP3 and PVR expression. HFFs were transfected with siRNA specific for ATR (siATR) (panels A-D), DNA-PK (siDNA-PK) (panels E-H), or a non-targeting siRNA (siCtrl), and then infected and harvested as described in Fig. S3. A) and E) Flow cytometry analysis of MICA, ULBP3 and PVR expression was performed as described in figure 1. Vertical dotted lines indicate the center of the peak for each ligand in

not infected-siCtrl transfected cells. All panels in A) or E) derive from the same experiment, representative of three. B) and F) The % of IE+ cells was analyzed by FACS on HCMV-infected cells stained intracellularly with a specific anti-IE mAb. C) and G) Cell culture supernatants were assayed for infectious virus production by plaque assay. D) and H) The levels of ATR or DNA-PK protein expression were assayed by immunoblot analysis with a specific antibody. Immunodetection of the p85 subunit of PI-3K was used as a control of protein loading. ns: not statistically significant difference with Student's t-test.

Supplementary Figure 4. Adenoviral-mediated overexpression of IE1 and IE2 proteins does not affect mRNA and cell surface expression of ULBP3. HFFs were transduced with adenoviral vectors (AdV) expressing IE1, IE2, or LacZ as a control, alone or in combination (total MOI 4 PFU/cell). Cells were harvested 24 h, 48 h or 72 h later, and analyzed for ligand mRNA and surface expression. A) Real-time PCR. Data from four experiments ± SEs, expressed as fold change units, were normalized with GAPDH and referred to not-transduced cells (-), considered as calibrators and set at 1. B) Cell surface expression levels of ULBP3 at 72 hpi, measured by FACS, are presented as MFI. Data from three experiments ± SEs. C) ULBP3 cell surface expression from a representative experiment performed at 72 hpi.

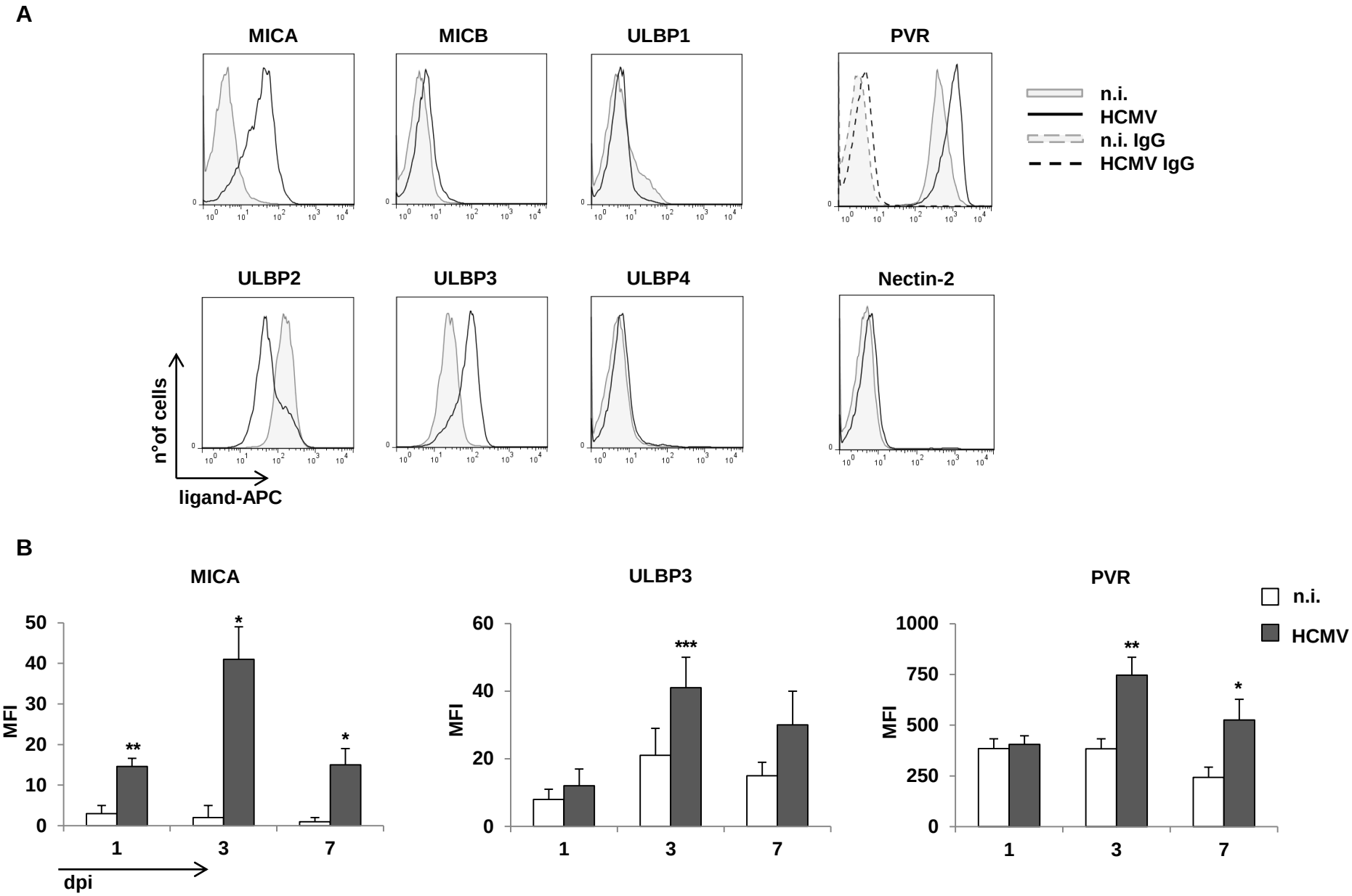
A
MICA
MICB
ULBP1
PVR
ULBP2
ULBP3
ULBP4
Nectin-2
n°of cells
ligand-APC
n.i.
HCMV
n.i. IgG
HCMV IgG
B
MICA
ULBP3
PVR
MFI
dpi
1
3
7
n.i.
HCMV

Figure 1

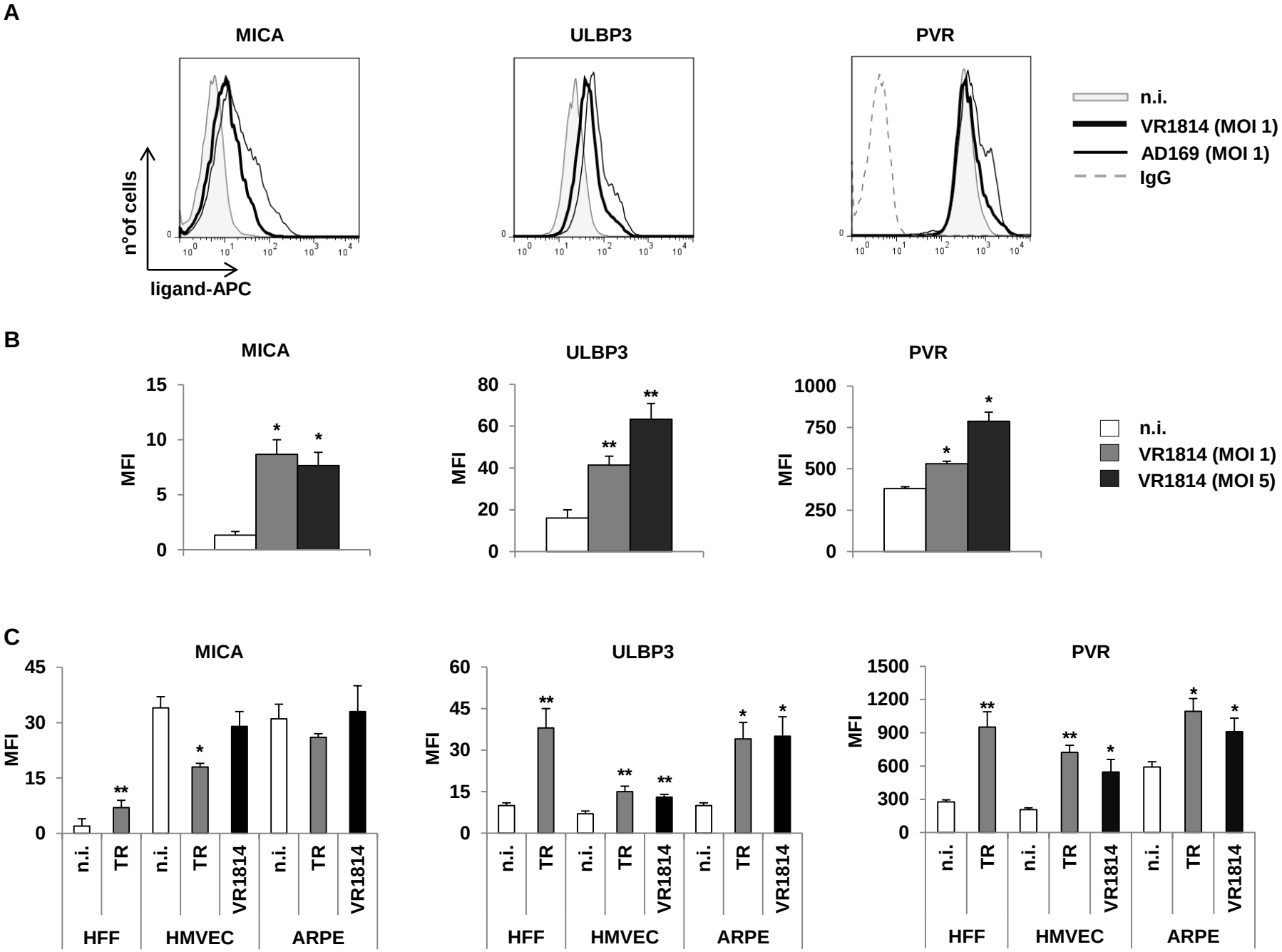
A
MICA
ULBP3
PVR
n°of cells
ligand-APC
n.i.
VR1814 (MOI 1)
AD169 (MOI 1)
IgG
B
MICA
ULBP3
PVR
MFI
n.i.
VR1814 (MOI 1)
VR1814 (MOI 5)
C
MICA
ULBP3
PVR
MFI
n.i.
TR
VR1814
HFF
HMVEC
ARPE

Figure 2

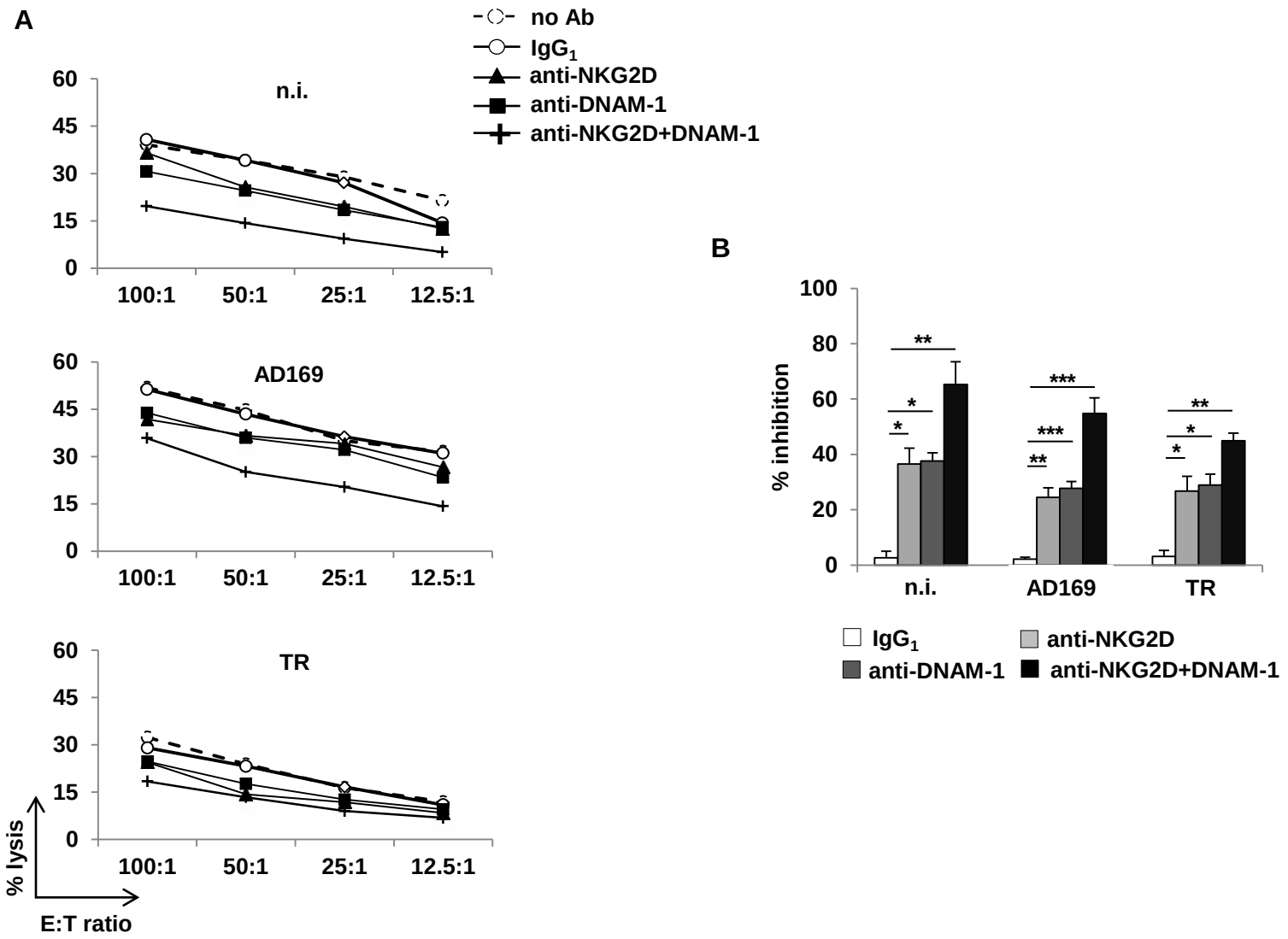
A
no Ab
IgG1
anti-NKG2D
anti-DNAM-1
anti-NKG2D+DNAM-1
n.i.
AD169
TR
60
45
30
15
0
100:1
50:1
25:1
12.5:1
% lysis
E:T ratio
B
% inhibition
100
80
60
40
20
0
n.i.
AD169
TR
IgG1
anti-NKG2D
anti-DNAM-1
anti-NKG2D+DNAM-1

Figure 3

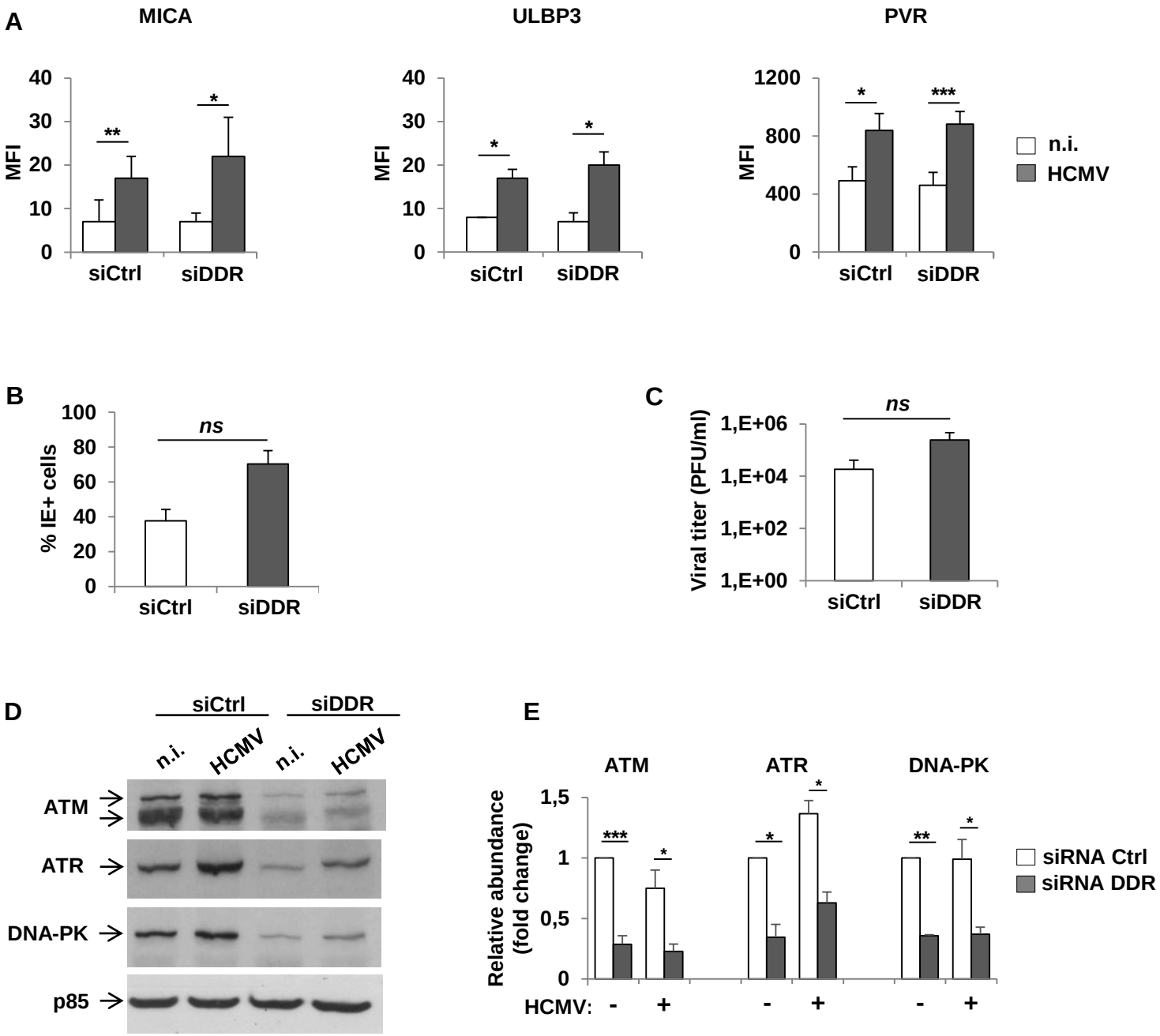
A
MICA
ULBP3
PVR
MFI
40
30
20
10
0
1200
800
400
**
*
***
siCtrl
siDDR
n.i.
HCMV
B
% IE+ cells
100
80
60
40
20
0
ns
C
Viral titer (PFU/ml)
1,E+06
1,E+04
1,E+02
1,E+00
D
siCtrl
siDDR
n.i.
HCMV
ATM
ATR
DNA-PK
p85
E
Relative abundance (fold change)
1,5
1
0,5
0
HCMV:
siRNA Ctrl
siRNA DDR

Figure 4

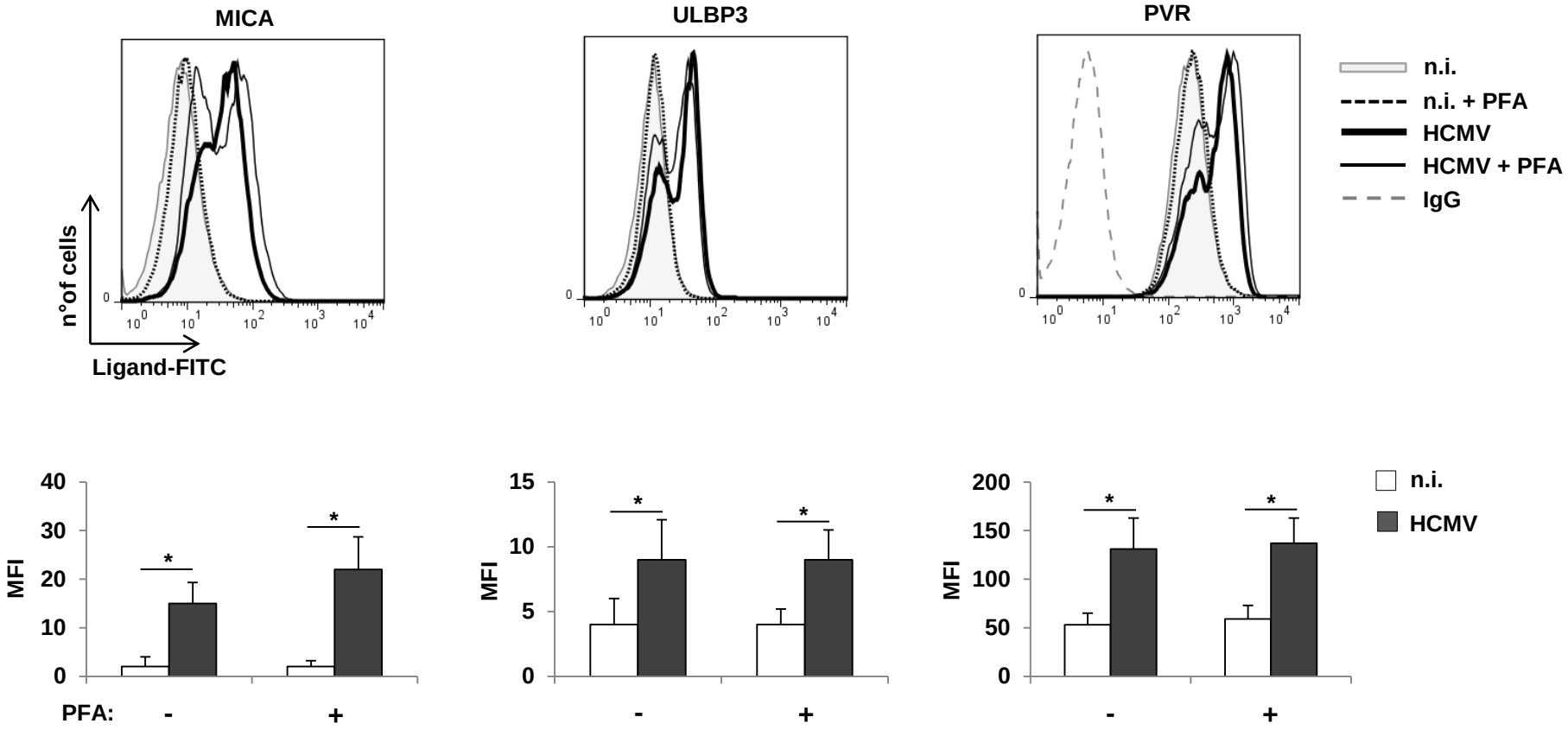
MICA
ULBP3
PVR
n°of cells
Ligand-FITC
n.i.
n.i. + PFA
HCMV
HCMV + PFA
IgG
MFI
PFA:
-
+
n.i.
HCMV

Figure 5

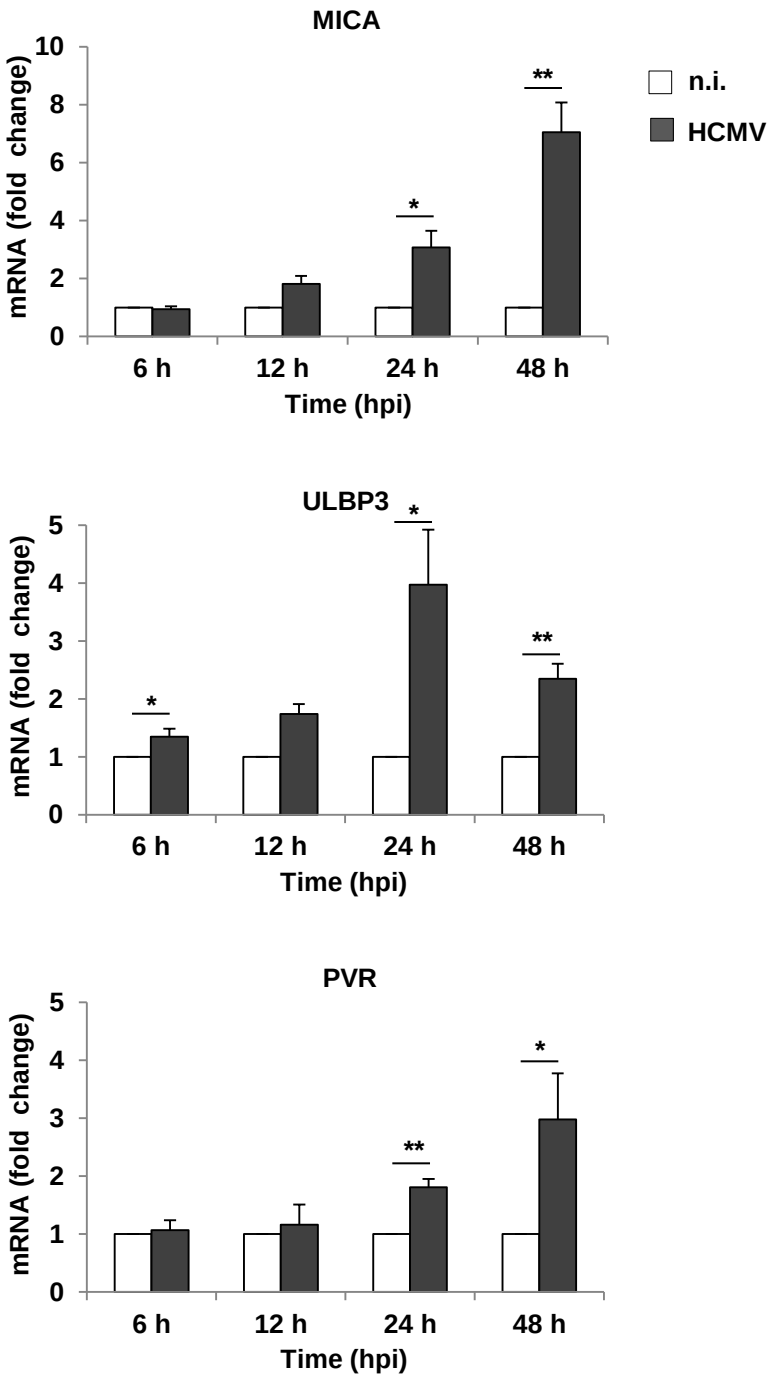
MICA
mRNA (fold change)
10
8
6
4
2
0
**
*
n.i.
HCMV
6 h
12 h
24 h
48 h
Time (hpi)
ULBP3
mRNA (fold change)
5
4
3
2
1
0
*
*
**
6 h
12 h
24 h
48 h
Time (hpi)
PVR
mRNA (fold change)
5
4
3
2
1
0
**
*
6 h
12 h
24 h
48 h
Time (hpi)

Figure 6

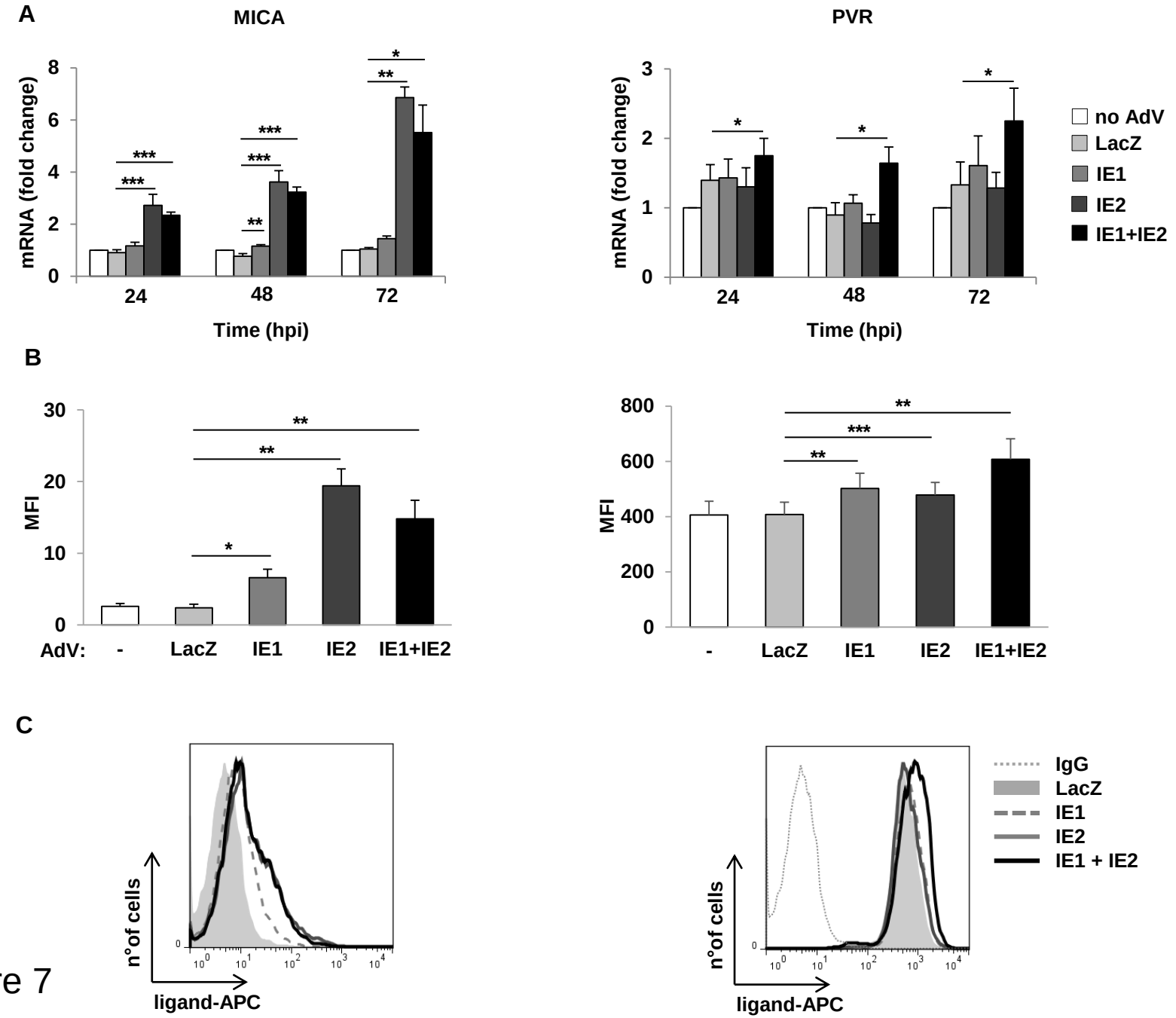
A
MICA
PVR
mRNA (fold change)
Time (hpi)
24
48
72
no AdV
LacZ
IE1
IE2
IE1+IE2
B
MFI
AdV:
-
LacZ
IE1
IE2
IE1+IE2
C
n°of cells
ligand-APC
IgG
LacZ
IE1
IE2
IE1 + IE2

Figure 7

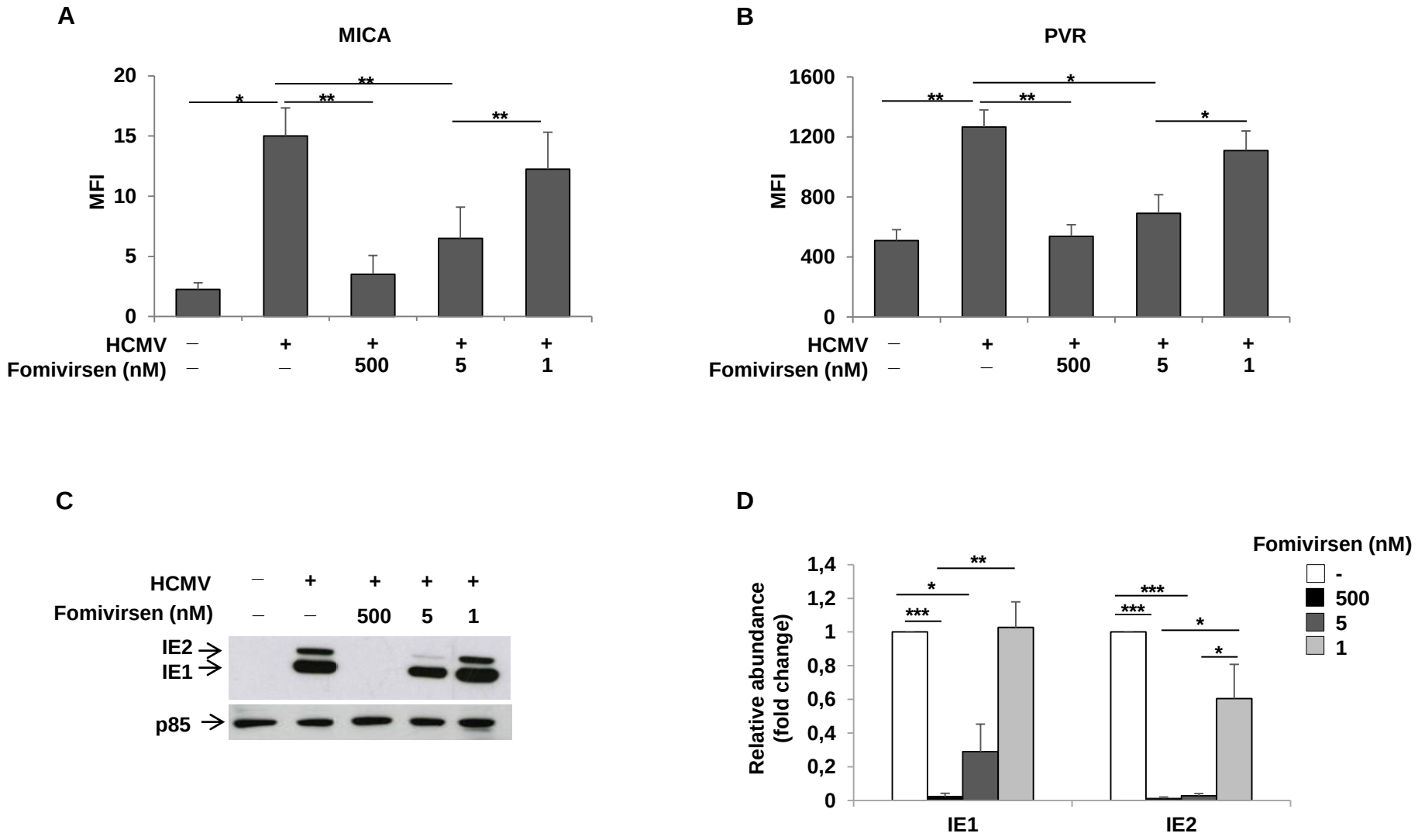
A
MICA
MFI
20
15
10
5
0
*
**
**
**
HCMV – + + + +
Fomivirsen (nM) – – 500 5 1
B
PVR
MFI
1600
1200
800
400
0
**
**
*
*
HCMV – + + + +
Fomivirsen (nM) – – 500 5 1
C
HCMV – + + + +
Fomivirsen (nM) – – 500 5 1
IE2
IE1
p85
D
Relative abundance (fold change)
1,4
1,2
1
0,8
0,6
0,4
0,2
0
*
**
***
***
***
*
*
IE1
IE2
Fomivirsen (nM)
-
500
5
1

Figure 8

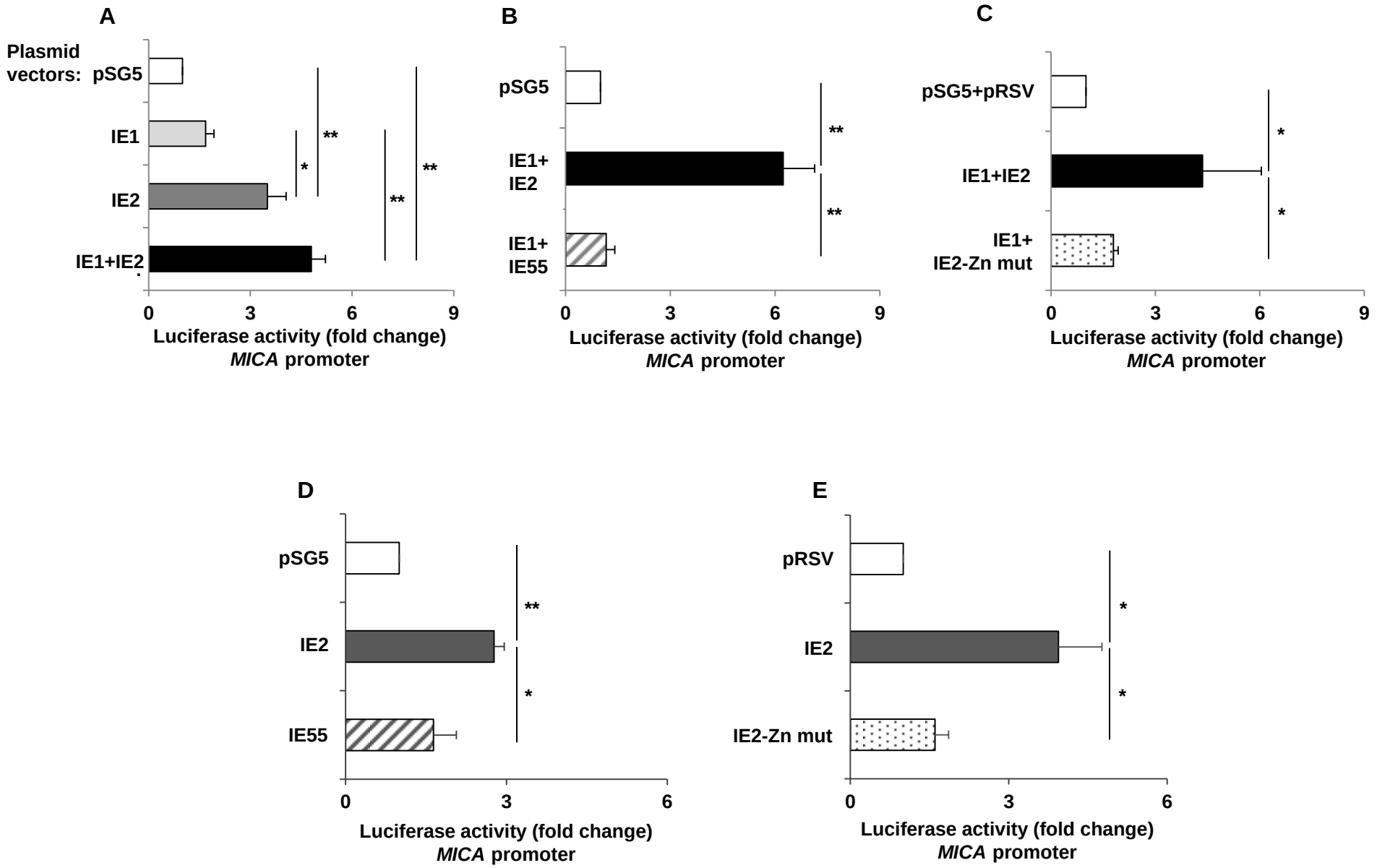
A
Plasmid vectors:
pSG5
IE1
IE2
IE1+IE2
**
*
**
**
0
3
6
9
Luciferase activity (fold change)
MICA promoter
B
pSG5
IE1+ IE2
IE1+ IE55
**
**
0
3
6
9
Luciferase activity (fold change)
MICA promoter
C
pSG5+pRSV
IE1+IE2
IE1+ IE2-Zn mut
*
*
0
3
6
9
Luciferase activity (fold change)
MICA promoter
D
pSG5
IE2
IE55
**
*
0
3
6
Luciferase activity (fold change)
MICA promoter
E
pRSV
IE2
IE2-Zn mut
*
*
0
3
6
Luciferase activity (fold change)
MICA promoter

Figure 9

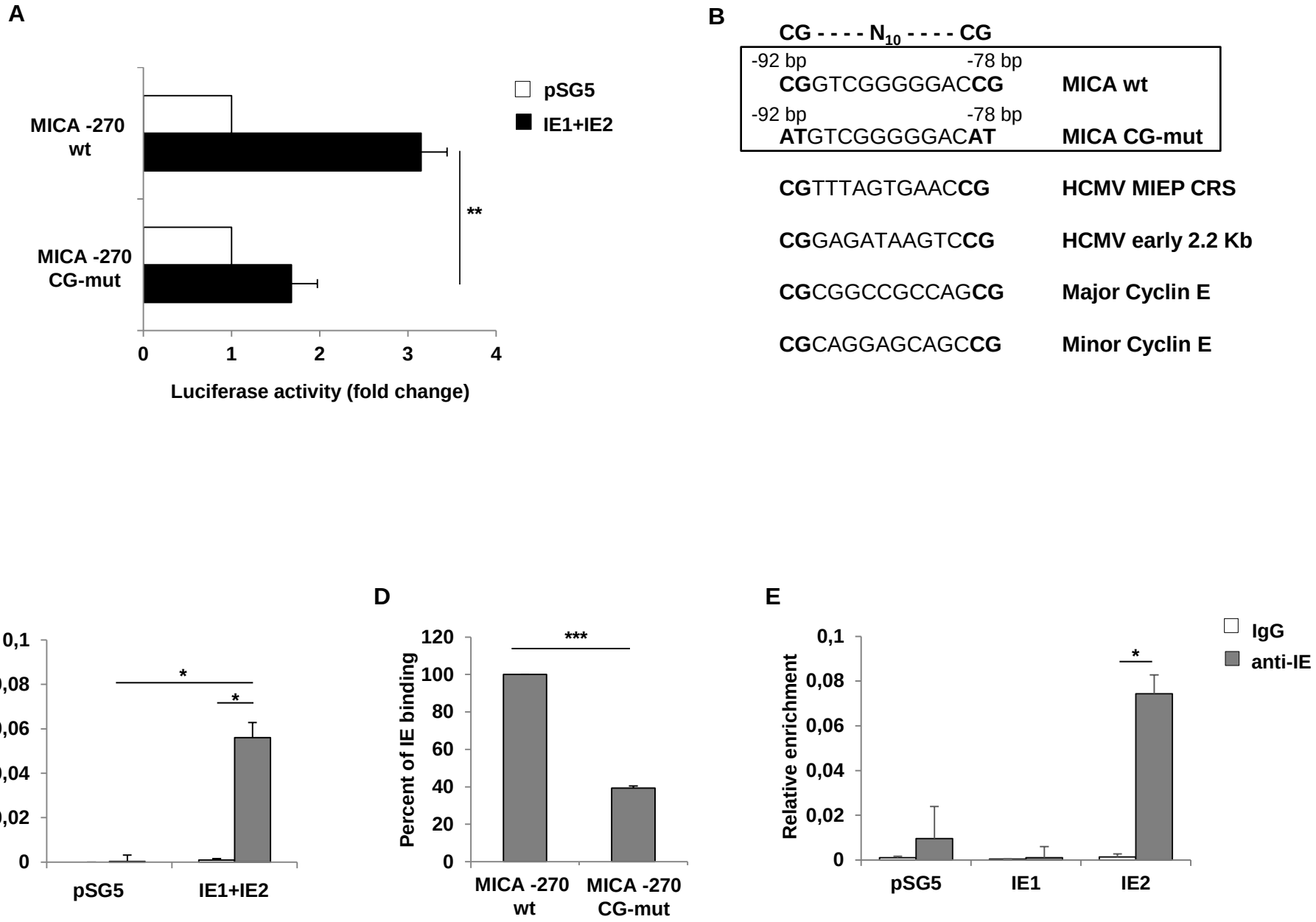
A
MICA -270 wt
MICA -270 CG-mut
pSG5
IE1+IE2
**
0
1
2
3
4
Luciferase activity (fold change)
B
CG - - - - N10 - - - - CG
-92 bp
-78 bp
CGGTCGGGGGACCG
MICA wt
-92 bp
-78 bp
ATGTCGGGGGACAT
MICA CG-mut
CGTTTAGTGAACCG
HCMV MIEP CRS
CGGAGATAAGTCCG
HCMV early 2.2 Kb
CGCGGCCGCCAGCG
Major Cyclin E
CGCAGGAGCAGCCG
Minor Cyclin E
C
Relative enrichment
0,1
0,08
0,06
0,04
0,02
0
*
*
pSG5
IE1+IE2
D
Percent of IE binding
120
100
80
60
40
20
0
***
MICA -270 wt
MICA -270 CG-mut
E
Relative enrichment
0,1
0,08
0,06
0,04
0,02
0
*
IgG
anti-IE
pSG5
IE1
IE2

Figure 10

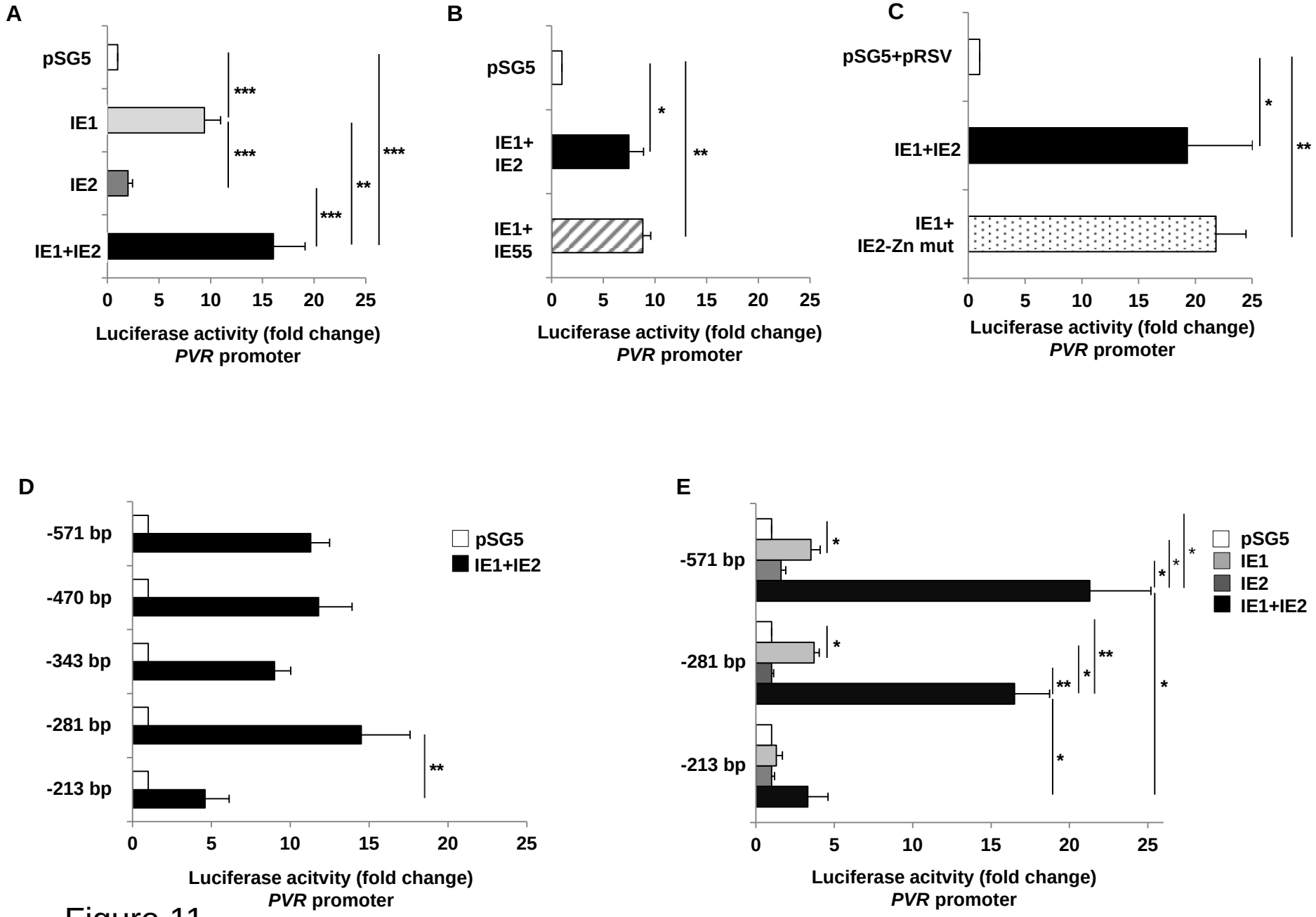
A
pSG5
IE1
IE2
IE1+IE2
***
***
**
***
0 5 10 15 20 25
Luciferase activity (fold change)
PVR promoter
B
pSG5
IE1+ IE2
IE1+ IE55
*
**
0 5 10 15 20 25
Luciferase activity (fold change)
PVR promoter
C
pSG5+pRSV
IE1+IE2
IE1+ IE2-Zn mut
*
**
0 5 10 15 20 25
Luciferase activity (fold change)
PVR promoter
D
-571 bp
-470 bp
-343 bp
-281 bp
-213 bp
pSG5
IE1+IE2
**
0 5 10 15 20 25
Luciferase acitvity (fold change)
PVR promoter
E
-571 bp
-281 bp
-213 bp
pSG5
IE1
IE2
IE1+IE2
0 5 10 15 20 25
Luciferase acitvity (fold change)
PVR promoter

Figure 11

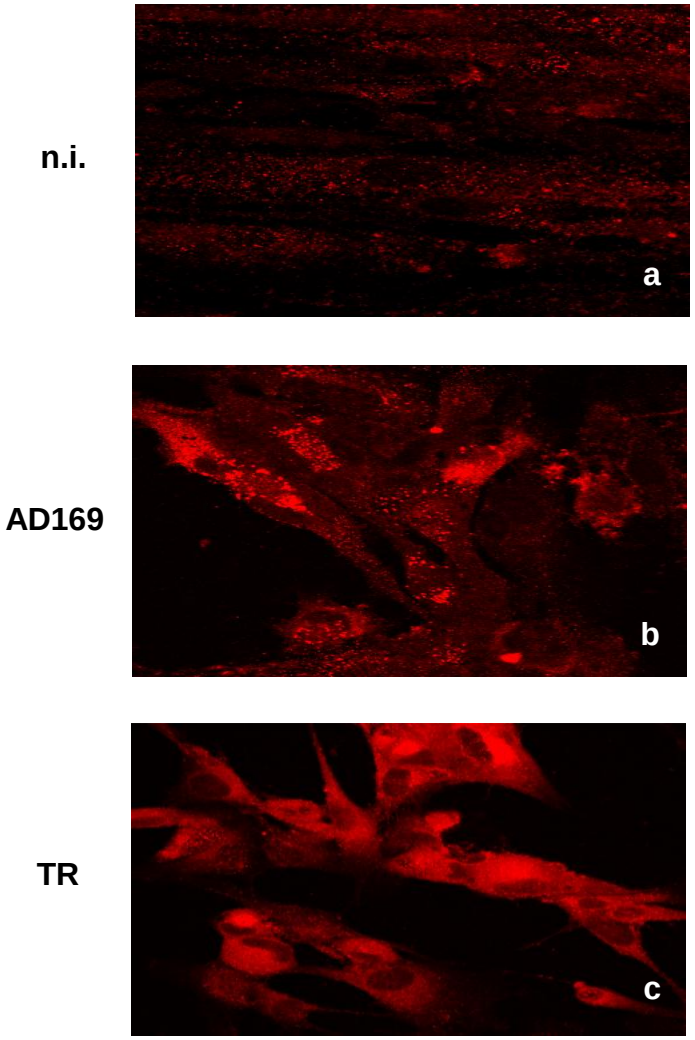

Supplementary Figure 1

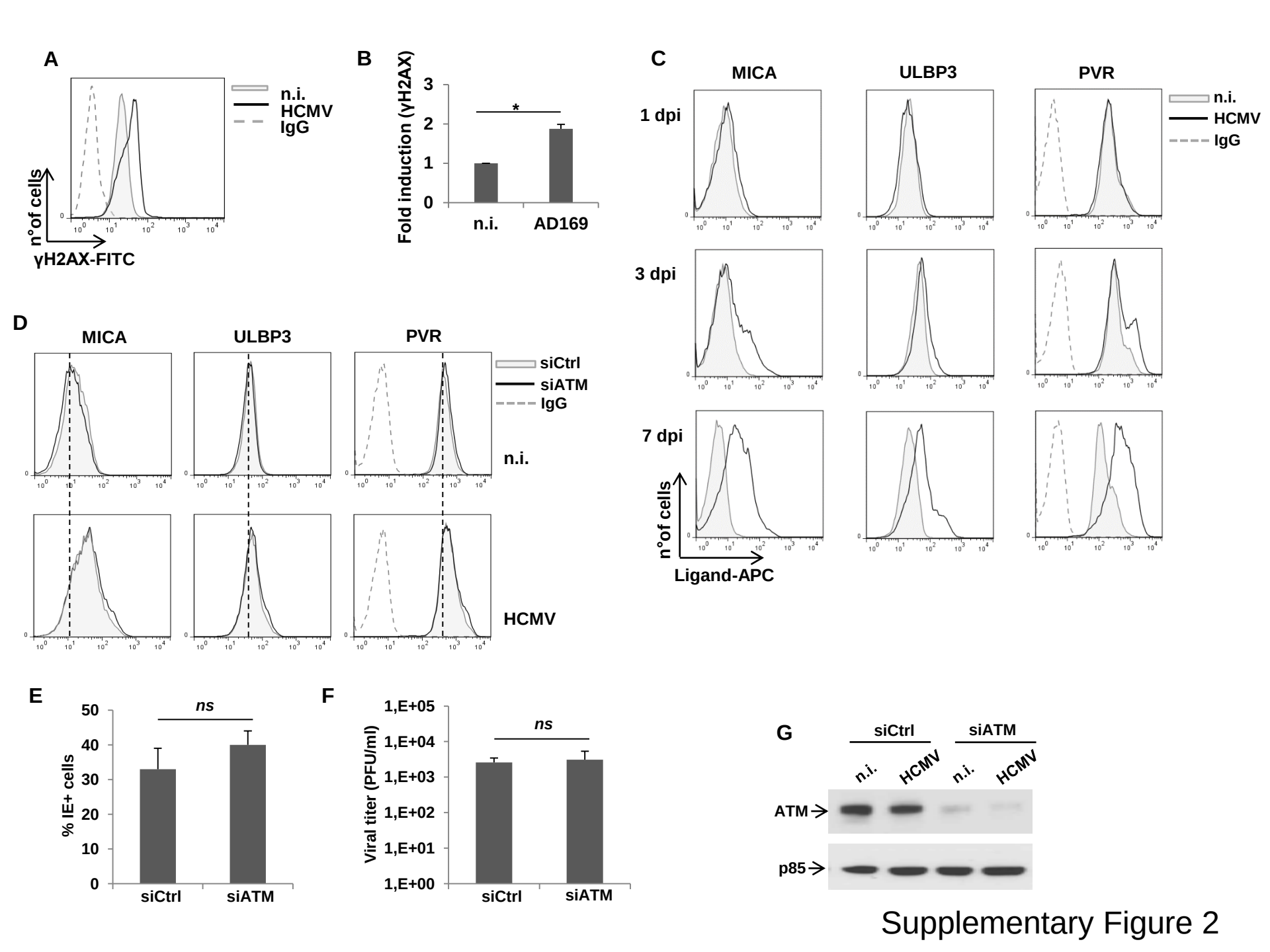

Supplementary Figure 2

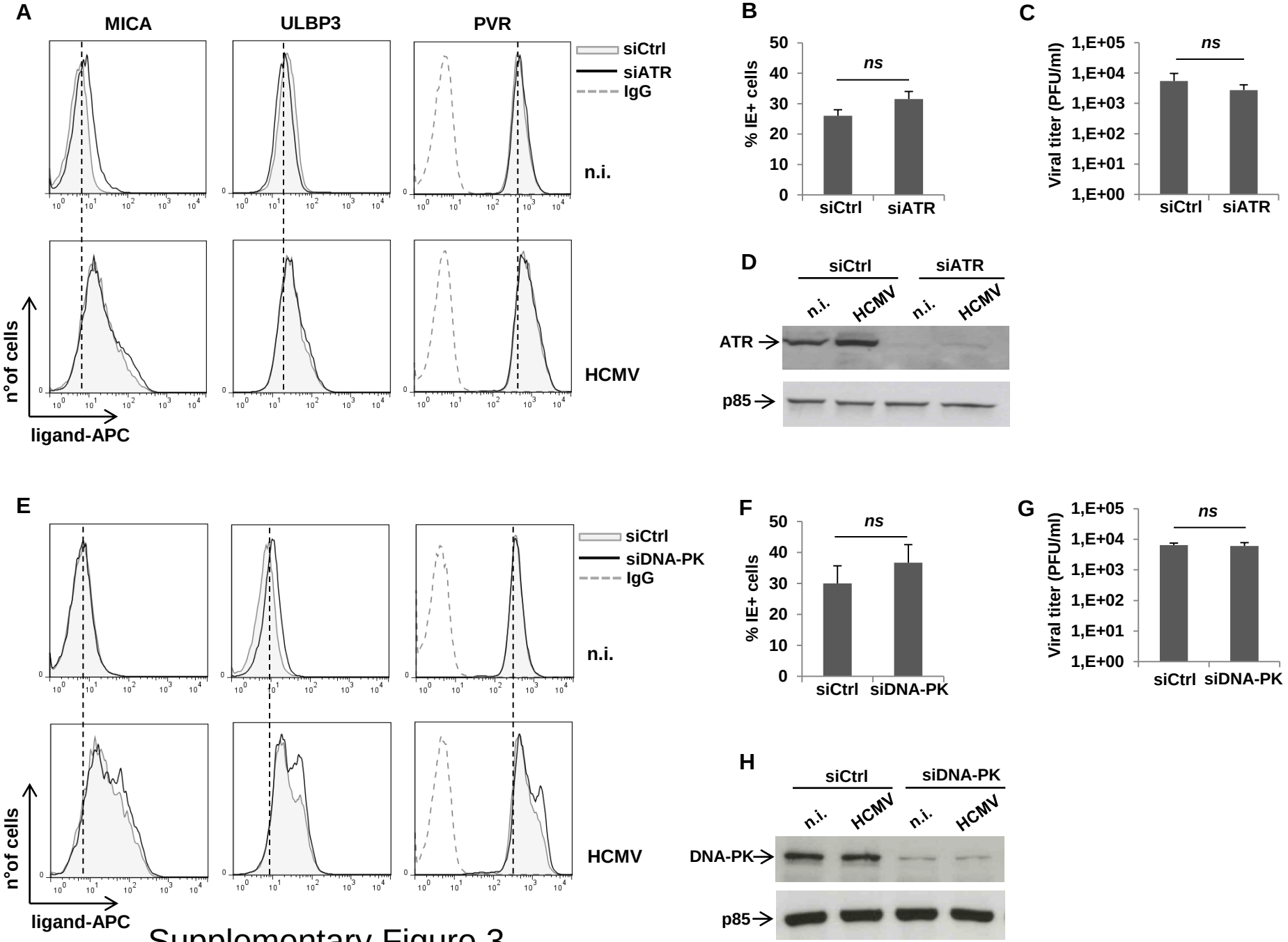

Supplementary Figure 3

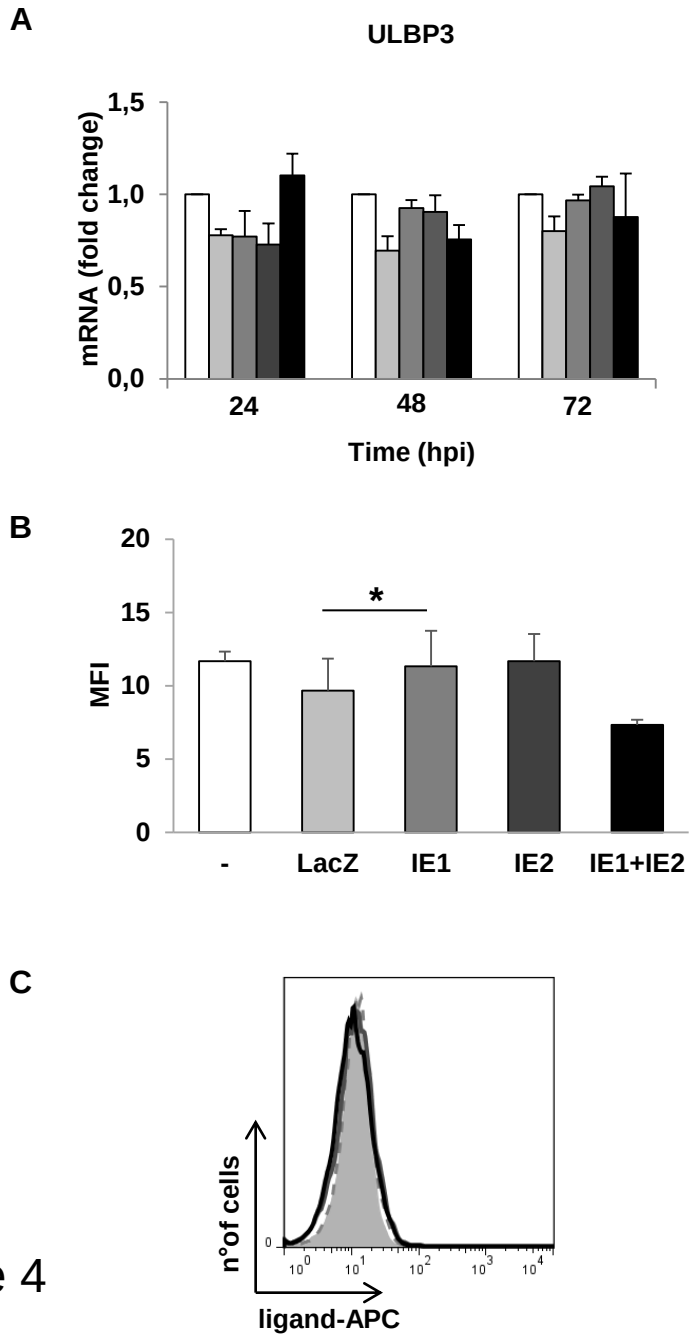

Supplementary Figure 4